MODELING THE EFFECTIVENESS OF POLYMER FLOODING FOR ENHANCING OIL RECOVERY COMPARED TO WATER FLOODING AND THE EFFECT OF RESERVOIR CHARACTERISTICS ON THEIR SWEEP EFFICIENCY

A Thesis

by

MIRNA ALAA MAHMOUD TAHA MAKLAD

Submitted to the Office of Graduate and Professional Studies of
Texas A&M University
in partial fulfillment of the requirements for the degree of

MASTER OF SCIENCE

Chair of Committee, Ahmed Abdel-Wahab
Co-Chair of Committee, Dominique Guérillot
Committee Member, Ahmed Abdala

Head of Department, Patrick Linke

December 2020

Major Subject: Chemical Engineering

Copyright 2020 Mirna Alaa Mahmoud Taha Maklad

ABSTRACT

The world has relied on the use of oil as its main source of energy for decades, whether it is to fuel the vehicles or to heat homes or to power industries; with the continuous increase in the global demand of oil, it is essential to work on maximizing oil production capabilities. Enhanced Oil Recovery (EOR) technologies are employed to improve sweep efficiency in oil reservoirs and increase oil recovery. Polymer flooding is an EOR technique that aims to increase the viscosity of water being injected to lower its mobility and displace more oil towards the production wells.

The purpose of this research is to investigate the effectiveness of polymer flooding in oil displacement, compared to water flooding and to examine the impact of reservoir characteristics on sweep efficiency, including reservoir porosity and reservoir permeability. An open source reservoir simulator has been used to model polymer flooding to evaluate its effect on oil recovery and compare it to pure water flooding, as well as investigate the effect of some reservoir characteristics such as porosity and permeability on oil recovery. Results will include changes in reduced oil saturation, reduced water saturation, and pressure for each injection process.

Conclusions deduced from the results obtained demonstrate more efficient oil recovery using polymer flooding when compared to pure water flooding. Polymer flooding may take longer time to flow due to being more viscous; however, eventually, it achieves more oil displacement towards the production wells. As for the reservoir characteristics, the higher porosity showed slower changes in oil saturation, water saturation and pressure, since it is initially storing more fluid as compared to the smaller pores, which are faster to drain out. The higher permeability demonstrated faster flow as oil saturation, water saturation and pressure changes were faster since

more oil was getting displaced easily and fast. Polymer flooding demonstrated the same change in saturation and pressure for the different porosity and permeability but at a slower pace.

ACKNOWLEDGEMENTS

I would like to thank my supervisor Dr. Dominique Guérillot, Professor at the Department of Petroleum Engineering in Texas A&M University in Qatar, for his constant guidance and kind support throughout the course of this research.

In addition I would like to also acknowledge the post docs Dr. Lei Ding and Dr. Jérémie Bruyelle for their assistance.

I want to also thank my committee members, Dr. Ahmed Abdel-Wahab and Dr. Ahmed Abdala for their continuous support.

Finally, a sincere appreciation goes to my family and friends for their constant encouragement and support.

Mirna, 2020

CONTRIBUTORS AND FUNDING SOURCES

Contributors

This work was supervised by a committee consisting of Professor Dr. Dominique Guérillot of the Department of Petroleum Engineering and Professor Dr. Ahmed Abdel-Wahab and Professor Dr. Ahmed Abdala of the Department of Chemical Engineering.

Dr. Jérémie Bruyelle assisted with running the simulation and Dr. Lei Ding provided beneficial feedback.

All other work conducted was completed independently by Mirna Maklad.

Funding Sources

This opportunity was made possible by the NPRP project [NPRP10-1214-160025] from the Qatar National Research Fund (a member of the Qatar Foundation) which provided a fellowship to support this graduate study.

The contents are the authors' responsibility and do not necessarily represent the official views of the Qatar National Research Fund.

NOMENCLATURE

Notation	Definition
λ_{phase}	Mobility of phase
μ_{phase}	Viscosity of phase
k	Absolute permeability
k_r	Relative permeability
k_{phase}	Effective permeability of phase
M	Mobility ratio
o	Oil
w	Water
f_w	Fractional flow of water
q_{phase} or Q	Volumetric flow rate/ Discharge rate
A	Cross sectional area
dp	Pressure gradient
dx	Length
z	Height
g	Gravitational acceleration
ρ	Density
h	Hydraulic head
∅	Porosity
q	Fluid source or sink
c_t	Total compressibility
v	Darcy flux
$P_{c_{ow}}$	Capillary pressure between oil and water phases
p_p	Pressure of phase p
S_p	Saturation of phase p
τ	Shear stress
γ	Shear rate
EOR	Enhanced Oil Recovery

TABLE OF CONTENTS

Page

LIST OF FIGURES

Page

1. INTRODUCTION

Since the 1950s, oil has started to globally dominate as a significant source of energy. It can be used to provide fuel for vehicles and planes, heat homes, supply power in industries, and manufacture chemical products like plastic (UKOG, 2020). In 2017, 28% of energy production in the United States was from crude oil and natural gas plant liquids (American Geosciences Institute, 2020). It is predicted that by 2030, 70% of the United Kingdom's supply of energy will still come from oil and gas (UKOG, 2020).

An oil field has an average lifespan of 15 to 30 years (Total Foundation, 2015). However, during that period, many factors can play a role in reducing oil production, such as a government's economic instability, which will affect the oil prices, or an unforeseen outbreak such as the current ongoing pandemic of COVID19, which is affecting the oil demand and consumption. Therefore, it is essential to work on recovering as much oil as possible before the oil field's lifespan ends. Primary recovery methods leave behind 85% to 95% of oil, while secondary recovery methods leave behind 50% to 80% of oil. Therefore improved oil recovery methods should be utilized to increase oil production (Envirofluid, 2014). The demand for oil continuously increases; it is predicted that there will be an increase in the global oil demand by 5.7 million barrels per day during the 2019 to 2025 period (IEA, 2020). According to IEA, in 2023 the oil demand will become 104.7 million barrels per day, an increase of 6.9 million barrels per day from 2018 (IEA, 2018). In 2018, the oil production to the consumption ratio in the world was 0.96, meaning the world consumes more than they produce (ENI, 2019).

There are three oil recovery techniques: primary recovery, secondary recovery and tertiary recovery. Primary recovery utilizes naturally existing energy in the reservoir; for instance, a

pressure gradient provides energy to move the fluids to the surface until the pressure starts to decline because of production. Secondary recovery is implemented when production slows down in primary recovery; this recovery augments the natural energy in the reservoir through injecting water or natural gas to help increase the pressure and displace the oil to the production wells (Zendehboudi et al., 2017). Water flooding is a common method for being inexpensive and abundant; its density is greater than that of oil. Hence it pushes the oil towards the production well. Tertiary recovery is used to further enhance oil production; it can vary from steam flooding, polymer flooding to CO_2 flooding (Zendehboudi et al., 2017).

For decades, Enhanced Oil Recovery (EOR) technologies have been optimized and applied in the field with the aim to increase recovery and improve sweep efficiency in oil reservoirs. Chemical injection is one of the main types of EOR, where a polymer augmented water gets introduced into a reservoir to increase the efficiency of water flooding. Field practices have shown polymer flooding increases recovery of 5 to 30% of original oil in place, OOIP (Abidin et al., 2012).

The objective of this research is to investigate the effectiveness of the use of polymer injection to enhance oil recovery compared to water flooding and to examine the impact of reservoir characteristics on sweep efficiency. An open source reservoir simulator developed by SINTEF will allow the modeling of polymer flooding versus water flooding into an oil reservoir to analyze phases' saturation and pressure change results to investigate if it improves the oil recovery. It will also allow the investigation of the effect of the reservoir characteristics, including the influence of porosity and permeability on oil recovery.

2. LITERATURE REVIEW

2.1 Polymer Flooding

The use of polymer in oil recovery first began in the 1960s in the United States; however, due to technical failure because of some loophole in the program used, the use of polymer flooding was decreased. In the 1980s, polymer EOR regained interest in China. Between the years 1987 and 1992, pilot tests on polymer injection were done in cooperation with IFP and Floerger Company, with the aim to increase oil recovery. Positive results were achieved, leading to extending this technique to the whole Daqing oilfield in China (Corlay et al., 1995). In 2004, it was widely used commercially. Incremental oil recovery from polymer injections leads to about an extra 10% of oil originally in place (OOIP). In the 1990s, the Courtenay oil field in France recorded extra oil recoveries from 5 to 30% after the use of polymer augmented water flooding (Thomas, 2016).

The higher viscosity of polymer flooding compared to water flooding increases the sweep efficiency and lowers the surface tension that inhibits oil flow in the reservoir. It gives better control of mobility between the hydrocarbons and injected water (Thomas, 2016). When a more viscous fluid than oil is injected, it will have lower mobility than that of the oil, resulting in oil displacement.

2.1.1 Mobility

The concept of mobility ratio, M, is linked to how polymers improve oil recovery (Standnes et al., 2014). Mobility ratio is the mobility of the displacing phase (water) to the mobility of the displaced phase (oil), as shown in Equation 1, where o and w refer to the phases oil and water, respectively. Phase mobility, λ_{phase}, is the ratio of the phase relative permeability, $k_{r(phase)}$, to

the phase viscosity, μ_{phase}. Viscosity indicates the fluid's resistance to flow, as it increases when the fluid is thicker and its mobility becomes lower.

$$M = \frac{\lambda_w}{\lambda_o} = \frac{\frac{k_{rw}}{\mu_w}}{\frac{k_{ro}}{\mu_o}} \qquad \text{Equation 1}$$

With the increased viscosity due to polymer flooding, the oil production rate is accelerated in flooded zones. Macroscopic sweep efficiency can also be improved as water mobility gets reduced due to adsorption in polymer flooded zones, which reduces viscous fingering as oil will flow more than water (Standnes et al., 2014). The effect of mobility ratio is shown through the principle of the Buckley-Leverett equation shown in Equation 2, where f_w is the fractional flow of water, q_w is the volumetric flow rate of water and k is absolute permeability. A is the cross sectional area, while dp is the pressure gradient and dx is the length (Buckley et al, 1941).

$$f_w = \frac{q_w}{q_o + q_w} = \frac{\frac{k_{rw}kA}{\mu_w}\frac{dp}{dx}}{\frac{k_{ro}kA}{\mu_o}\frac{dp}{dx} + \frac{k_{rw}kA}{\mu_w}\frac{dp}{dx}} = \frac{\frac{k_{rw}}{\mu_w}}{\frac{k_{rw}}{\mu_w} + \frac{k_{ro}}{\mu_o}} = \frac{M}{1+M} \qquad \text{Equation 2}$$

If M is higher than 1, it is undesirable as water has higher mobility than oil and may result in an early water-breakthrough. If M is less than 1, it is favorable as oil has higher mobility and is produced faster than water as water acts in a piston-like manner to displace oil (Standes et al, 2014). For a two-dimensional heterogeneous reservoir, a suitable M value would be around 0.1 to 0.3 (Sorbie, 1991).

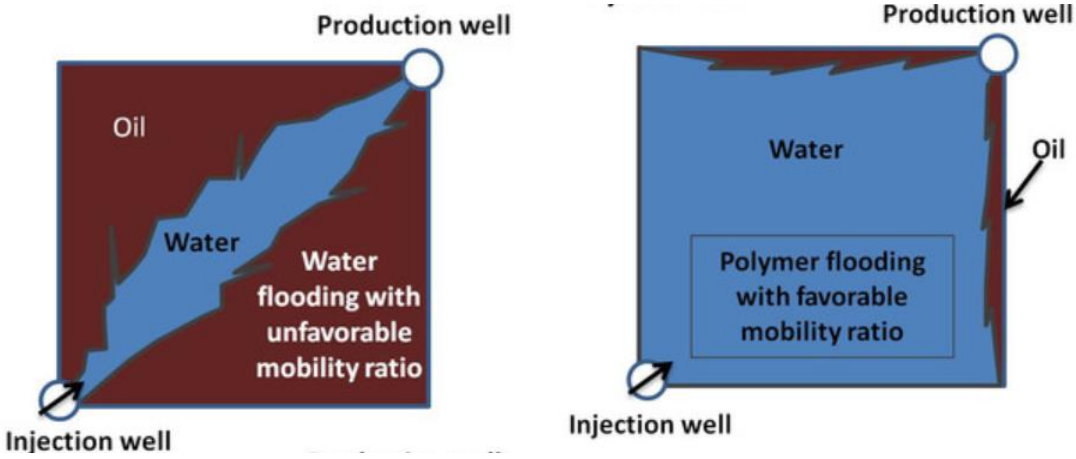

Figure 1: Water flooding (left) vs Polymer flooding (right) (Adapted from: Zerkalov, 2015)

Water density is higher than oil density, which makes water flooding effective in displacing oil; however, as shown in Figure 1, the water flooding case showed an early breakthrough of water as it cuts through the oil and bypasses sections of the reservoir leaving behind more oil in place. The mobility ratio in this case is unfavorable as it is larger than 1 and promotes the fingering effect seen. The polymer flooding case shows a favorable mobility ratio. With a higher viscosity, the polymer injection improves the sweep efficiency and displaces more oil towards the production well.

2.1.2 Types of Polymers

Two main types of polymers are utilized in the process of polymer flooding, a synthetic polymer and a biopolymer, to increase the injected fluid's viscosity which influences mobility to improve oil recovery. The most commonly used synthetic polymer is the hydrolyzed polyacrylamide (HPAM) and the most popular biopolymer is Xanthan Gum, which is produced by the fermentation of the bacterium Xanthomas (Firozjaii et al, 2019). Their structures are as shown

in Figure 2. HPAM is more widely used for its low cost, good viscosity-enhancing performance and huge commercial availability (Preux, 2018).

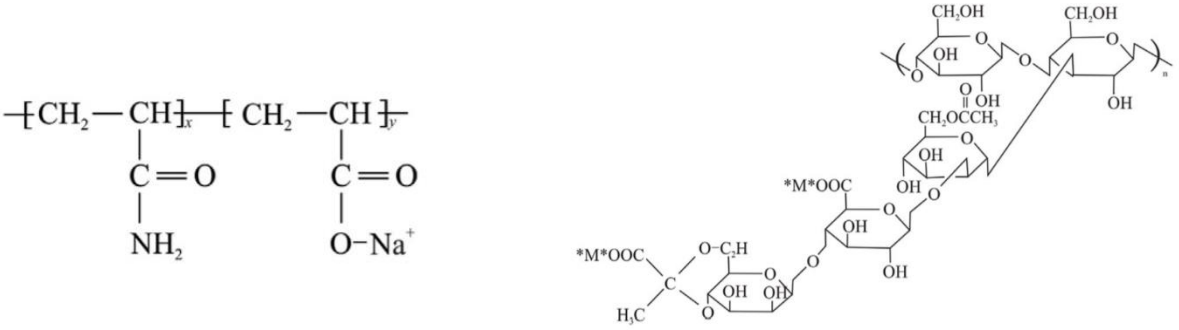

Figure 2: HPAM structure (left), Xanthan Gum structure (right) (Adapted from: Firozjaii et al, 2019)

Other types of polymer flooding include the use of alkali-surfactant polymers and surfactant polymers, which are used to recover residual oil and reduce the interfacial tension between oil and water (Thomas, 2016). Surfactants can generate emulsions, while alkali can generate soaps when it reacts with the crude oil, which can adsorb at the oil-water interface. Alkali can also adjust salinity (SNF, 2012).

Some polymers are being designed to overcome the limitations of the conventionally used polymers, HPAM and Xanthan, discussed in section 2.1.4. Thermoviscosifying polymers (TVPs) have reported increasing viscosity and elastic modulus with increased temperature (Wang et al., 2012). They represent a potential alternative to HPAM to be used in high temperature and high salinity reservoirs, however they are of low molecular weight which needs to be increased. A biopolymer that is being investigated as a potential alternative is Schizophyllan, which showed a

stable viscosity at a salinity of 220 g/L and a temperature of 135℃, however its production is uneconomical in many cases (Firozjaii et al., 2019).

2.1.3 Polymer Rheology

The rheology of a fluid describes its flow behavior. The addition of polymer to water to form a polymer solution changes the viscosity, which is considered an important rheological property of the polymer solution. The polymer solution is considered a non-Newtonian fluid, hence its viscosity depends on shear stress and shear rate, as shown in Equation 3, where τ is shear stress, γ is shear rate and μ is viscosity (Firozjaii et al, 2019).

$$\mu = \frac{\tau}{\gamma} \qquad \text{Equation 3}$$

Most polymer solutions exhibit shear thinning, meaning that its viscosity decreases as the shear rate increases. It can act as a Newtonian fluid when the shear rate is lower or higher than a certain point as shown in Figure 3 below. Specifically HPAM polymer solutions exhibit Newtonian behavior for flux values of 0.01 to 0.2 ft/day in vertical injector and 0.2 ft/day in horizontal well (Seright, 2010).

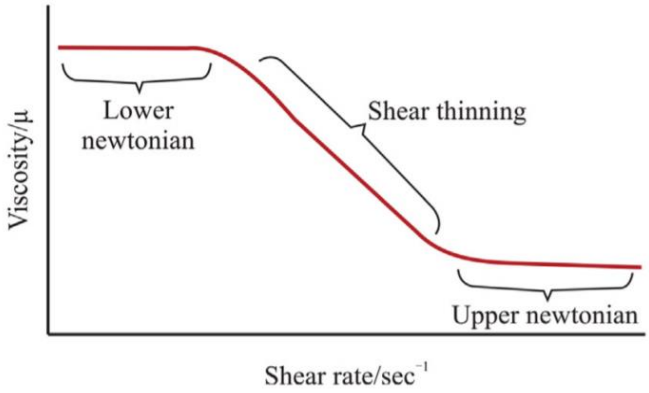

Figure 3: Log-log plot of viscosity vs. shear rate of shear thinning fluid (Adapted from: Firozjaii et al, 2019)

Besides the effect of shear rate on the viscosity of the polymer solution, the polymer concentration can also have an effect. A high concentration of polymer can cause high pressure during injection. Therefore it is better to use a polymer of high molecular weight to achieve higher viscosity for a lower polymer concentration. The size of the polymer molecule should be considered to fit into the pore space.

2.1.4 Affecting Factors

Several factors can affect the rheology behavior of a polymer solution, such as temperature, microbial activity, shear rates and salinity. HPAM hydrolyzes at high temperature and high salinity, which decreases its viscosity and affect its efficiency. The maximum temperature HPAM can withstand can be up to 120°C (Seright et al., 2010). As the molecular weight of the HPAM increases, its viscosity increases if the other factors are constant; however, the easier it can degrade from the high shear rates near the well area (Sorbie, 1991). At low concentration, high molecular HPAM is required for a higher viscosity (Nasr El-Din et al., 1995). The molecular weight of HPAM can vary up to 30 million Daltons (Abidin et al., 2012).

The biopolymer Xanthan Gum is more expensive and can also degrade at high temperature and high salinity, however, it is more stable than HPAM (Firozjaii et al, 2019). Xanthan is stable

for temperatures below 90°C. Salinity can deform the polymer shape from inflated to spherical (Sorbie, 1991).

SNF Floerger is an infamous company that manufactures polyacrylamide-based polymers to be used in enhanced oil recovery among other applications. According to SNF there are some preferred conditions for some of the reservoir properties such as a permeability range between 50 mD to 10 D, temperature up to 120°C and the lithology to be preferably sandstone. The oil viscosity can range from 10 to 10,000 cP, the oil saturation to be higher than 20% and the oil gravity to be higher than 15° API. The salinity is preferred to be lower than 250,000 TDS (SNF, 2012).

As mentioned by Abidin et al. (2012), since there is less water production and more oil production in polymer flooding, water flooding costs more. The efficiency of the process is estimated to be in the range of 0.7 to 1.75 lb of polymer per bbl of incremental oil production (Abidin et al., 2012). According to Seright (2010), oil prices are in the range of $70 per bbl and the HPAM polymer prices are in the range of $0.9 to $2 per lb.

2.1.5 Polymer Flooding Applications

Standnes et al. (2014) compiled data taken from polymer flooding projects carried out over the last 50 years, where 40 projects were considered a success. The data based on the successful projects included polymer efficiency range of 0.02 to 12.5 Sm^3 per kg polymer injected, an average permeability of 563 mD, and a polymer concentration of 770 ppm. The data also included a resistance factor (RF) range of 5 to 12 and a residual resistance factor (RRF) range of 1 to 8. RF is the ratio between aqueous phase mobility without polymer to aqueous phase mobility with the polymer. RRF is the aqueous phase mobility before polymer injection to aqueous phase mobility after the polymer injection. The successful projects report a polymer retention range of 5 to 60

μ_g/g and a well spacing range of 15 to 450 m (most were above 400 m). The temperature average was between 24 to 85°C, and the average oil viscosity was 44 cP.

According to Seright's (2016) research on polymer flooding viscosities and past industrial bank sizes, as shown in Figure 4, some EOR projects in Canada inject 30 cP polymer solutions to displace 1000 to 3000 cP oil, while in China's Daqing oilfield they inject 150 to 300 cP polymer solution to displace 10 cP oil. Many reasoning can be deduced to why different reservoirs have different polymer injection characteristics, such as economic limitations, different mobility ratios or limitation on the viscosity allowed to be injected (Seright, 2016).

China's Daqing oilfield is a heterogeneous sandstone reservoir with a depth of 1000m and temperature of 45°C. Oil viscosity is 9 cP and formation water total salinity ranges from 3000 to 7000 mg/L (Wang et al., 2008). Wang et al. (2011) reported that in Daqing over 5600 wells were injected with 150 to 300 cP HPAM solution (with molecular weight of 20 to 35 million g/mol) to displace 9 cP oil from 500 to 800 md rock, which was about 20% original oil in place (OOIP). Daqing oil field showed approximately 12% incremental oil recovery (Thomas, 2016). Concluding from 12 years of experience at Daqing oil field, the preferable polymer molecular weights varies from 12 to 38 million Daltons, a value around 0.7 PV for the polymer injection volume and a polymer concentration around 1000 mg/L (Wang et al., 2008). For a 250m well spacing, the optimum polymer injection rate ranges between 0.14 to 0.16 PV per year (Wang et al., 2008). According to Standnes et al. (2014), collective findings on preferred characteristics for successful oil recovery, the polymer injected viscosity is 28 cP.

Oman's Marmul oil field is a heterogeneous sandstone reservoir with a temperature of 46°C and the oil is 22 API with a viscosity of 90 cP. The formation water total salinity is around 3000 ppm and the polymer injection rate is 13000 m^3/day at a viscosity of 15 (9 in-situ) cP and 1000

ppm concentration (Alsaadi, 2012). Marmul's oil field showed about 10% incremental oil recovery (Thomas, 2016). Angola's Dalia oil field is a sandstone reservoir with permeability higher than 1D, temperature of 50°C and 21 to 23 API oil with viscosity varying between 3 to 7 cP (Morel, 2008). In Dalia, a polymer concentration of around 900 ppm is injected at a rate of 5 t/d of polymer and was stopped after injecting 7 million bbl (Carpenter, 2016). Dalia's oil field showed about 3 to 7% incremental oil recovery (Morel, 2008). According to Seright (2010), previous polymer floods used polymer concentrations of 1000 or less ppm to displace oil that had viscosities less than 50 cP.

Field	C_{poly}, ppm	μ_{poly}, cp	μ_o @ Res. T, cp	Endpoint M	k_{cont}	μ_{poly} [M*k_{cont}]	Bank size, PV	Graded?
Daqing, China (1996-~2008)	1000-1300	40-50	9-10	9-10	4:1	~1	~1	Mixed
Daqing, China (~2008-2016)	2000-2500	150-300	9-10	9-10	4:1	3-8	0.4-1.2	Mixed
Gudao/Shengli, China	2000	25-35	50-150				0.4-0.6	
Shengtao/Shengli, China	1800	30-50	10-40				0.4-0.6	
ShuangHe, China	1090	93	7.8		4:1		0.4	yes
Bohai Bai, China	1200-2500	98	30-450		4:1		0.11-0.3	
Pelican Lake, Canada	600-3000	13-200	~1650	~165	4:1	0.02-0.3	0.5-2	
East Bodo, Canada	1500	50-60	417-2000	~42				
Mooney, Canada	1500	20-30	100-250					
Seal, Canada	1000-1500	25-45	3000-7000					
Suffield Caen, Canada	1300	32	69-99	44-64	4:1	~0.2	0.6	
Wainwright, Canada	2100-3000	25	100-200				0.5	yes
Dalia, Angola	900	3	1-11		10:1		0.5	yes
Diadema, Argentina	1500-3000	15-40	100	80	9:1	~0.06	0.8	
El Corcobo, Argentina	1000	20-25	160-300					
Matzen, Austria	900	10	19	17				yes
Canto do Amaro, Brazil	1000	30	50	12			0.1	
Carmopolis, Brazil	500	40	10.5	3			0.16	
Buracica, Brazil	500	10	7-20	2-5			1.1	
Bockstedt, Germany	300 (biopoly)	25	11-29		3:1			
Mangala, India	2000-2500	20	9-22	36	10:1	~0.06	0.8	yes
Marmul, Oman	1000	15	80-90	~40	10:1	~0.04	1	
Tambaredjo, Suriname	1000-2500	45-140	325-2209	40-50	12:1	~0.4		

Figure 4: Recent polymer flooding projects (Adapted from: Seright, 2016)

2.2 Reservoir Geology

An oil reservoir is a porous rock that contains crude oil trapped within. Sedimentary rocks, such as carbonates and sandstones are among the most common type of oil reservoirs.

2.2.1 Reservoir Heterogeneity

Reservoir heterogeneity is the variations in the rock properties due to its formation process including sedimentation, diagenesis and erosion. These variations can also affect the reservoir permeability (Schlumberger, 2020).

Reservoir heterogeneity can affect the behavior of fluid flow, thus can affect the reservoir producibility (Corvi et al., 1992). It is important to consider the heterogeneities of a reservoir to obtain realistic production predictions (Guérillot et al., 1990). Heterogeneity can be classified according to scale. The smallest scale is microscopic heterogeneity which considers grain-scale features such as the porosity, permeability and the grain-size distribution (Harraz, 2019). The heavy crude oil recovered from reservoirs is often referred to as black oil.

2.2.2 Reservoir Wettability

A significant characteristic that can influence the reservoir performance during oil recovery techniques is the reservoir wettability. According to Schlumberger (2017), wettability is the solid's preference to be in contact with one fluid rather than another. An oil-wet reservoir prefers to be in contact with oil and a water-wet reservoir prefers contact with water.

The residual oil saturation, S_{or}, measured after waterflooding demonstrates the effect of wettability on the amount of oil produced at the pore level. The fluid that occupies the outside of the pores and is in contact with the rock surface is the wetting fluid. A water-wet reservoir has water on the outside of the pore in contact with the surface and oil at the center of the pore, while

in an oil-wet reservoir, oil is in contact with the surface and water is in the center of the pore. Oil recovery is higher in water-wet reservoirs because it is easier for the fluid in the center of the pore to flow than the fluid outside the pore as it is held by surface tension. In mixed-wet reservoirs, smaller pores are water-wet filled with water and large pores are oil-wet filled with oil (Schlumberger, 2017).

2.2.3 Capillary Pressure

Capillary pressure can be written as the pressure difference between the two phases, where the wetting fluid pressure is subtracted from the non-wetting fluid pressure. For instance, for a water-wet reservoir, the capillary pressure is as shown in Equation 4. In water-wet reservoirs, oil gets displaced by water through an imbibition process (Dake, 1978). As the pressure difference increases between the resident water and buoyant oil, water saturation will be reduced as the oil will increasingly be able to enter narrow paths.

$$P_{c_{ow}}(S_w) = P_o - P_w \qquad \text{Equation 4}$$

Capillary pressure can influence the movement and direction of the liquids, thus plays a role in the fluid distribution in the reservoir.

2.2.4 Relative Permeability

Permeability describes the ability of the reservoir to permit the flow of a fluid. According to Darcy's Law, as demonstrated in Equation 6, permeability depends on factors including volume of fluid flow per time, cross sectional area, pressure gradient, length of the rock sample, and the fluid viscosity. The connecting passageways between pores can affect permeability and flow rate, as it may be narrow or blocked, thus reducing the flow and decreasing permeability. Absolute

permeability, k, measures the ability to flow fluids when a single fluid exists in the rock. Effective permeability is measured when two fluids, such as water and oil are flowing through the rock, it measures the ability to preferably transmit a fluid while another is present. The effective permeability of oil is written as k_o. Relative permeability, $k_{r(phase)}$, is the ratio of effective permeability of a specific phase at a specific saturation to that phase's absolute permeability at total saturation (Schlumberger, 2020). Relative permeability of a single fluid would be 1.

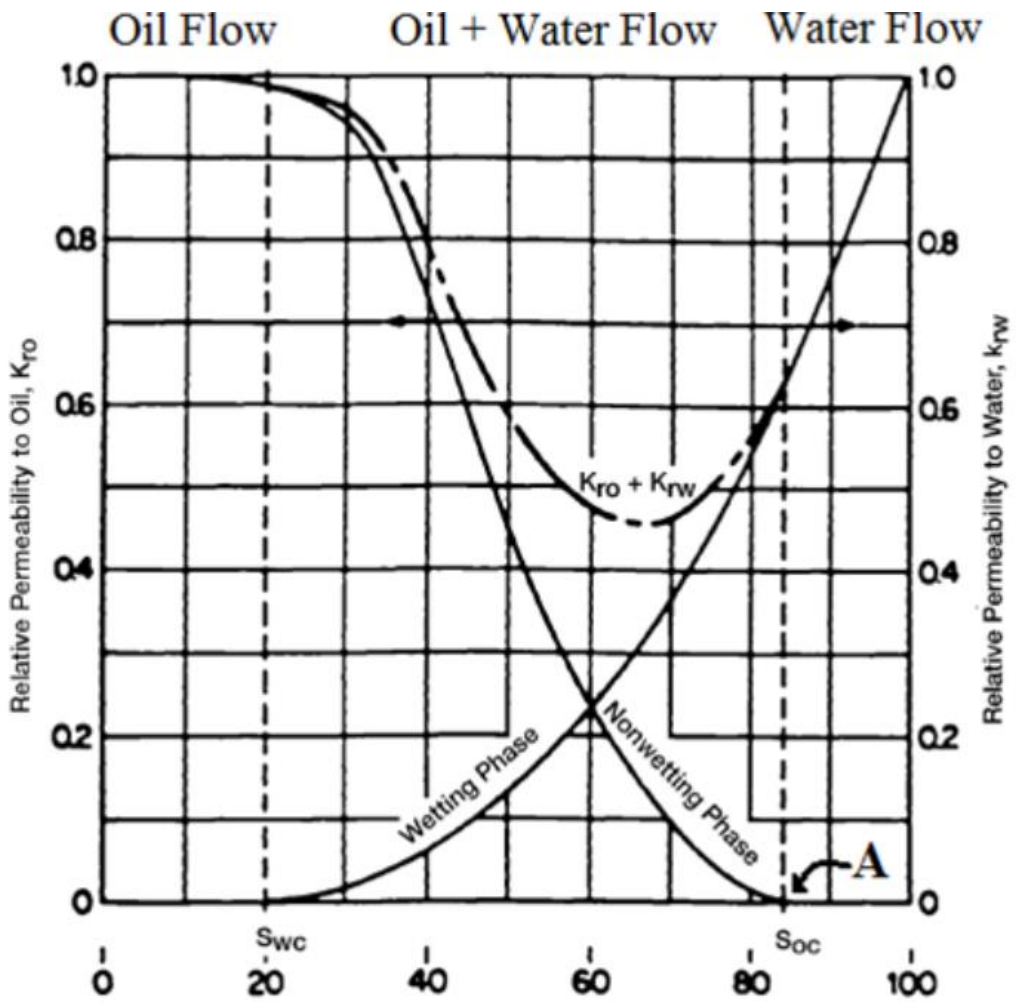

Figure 5: Relative permeability curve for a water-wet reservoir (Adapted from: PERM, 2020)

Figure 5 demonstrates a standard curve that plots the relative permeability of two fluids as a function of water saturation. In a typical relative permeability curve, at low water saturation, only oil will flow. S_{wc} is the connate water saturation, which is the amount of water that adsorbs onto the rock surface divided by pore volume. As water saturation increases, the relative permeability of oil decreases until a certain point is reached where both oil and water flow. The oil flow decreases as water flow and water saturation increases. At some point of water saturation, when critical oil saturation, S_{oc}, is reached oil stops to flow and only water continues to flow within the reservoir and water saturation continues to increase.

2.2.5 Saturation

Saturation is the fraction of the pore volume occupied by phase, so for instance water saturation is the relative amount of water in the rock pores as a percentage of volume (Schlumberger, 2020). In multiphase, the void space can be filled with more than one fluid, such as oleic, aqueous or gaseous phases, as long as the sum of all saturations equal 1. For two phases of oil and water, their saturation sum is as shown in Equation 5.

$$S_w + S_o = 1 \qquad \text{Equation 5}$$

2.3 Relevant Equations

2.3.1 Darcy's Law

The French hydraulic engineer, Henry Darcy, designed an experiment to define an equation that will describe the flow of fluid through a porous medium like a rock. The experiment consisted

of a vertical tank filled with sand, with water being injected at the top and flowing out of the bottom as shown in Figure 6.

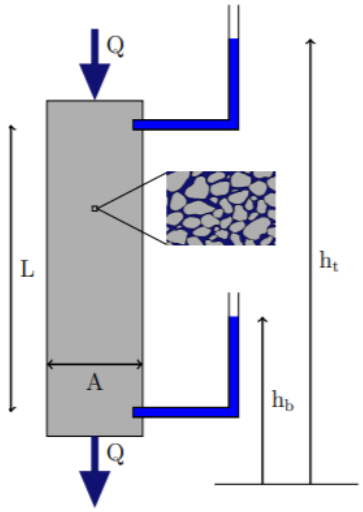

Figure 6: Illustration of Darcy's experiment (Adapted from: Lie, 2019)

From the experiments Darcy established a relationship between the discharge rate Q [m^3/s], the cross sectional area A [m^2], the difference in hydraulic head (h_t-h_b) [m] which is height of the water and the flow length of the tank L [m] as demonstrated in Equation 6 (Lie, 2019).

$$v = \frac{Q}{A} = k\frac{h_t - h_b}{L} \qquad \text{Equation 6}$$

The Darcy flux is v [m/s] and the hydraulic conductivity is $k = \frac{\rho g K}{\mu}$, where g [m/s^2] is gravitational acceleration, μ [kg/ms] is dynamic viscosity, and K [m^2] is the absolute permeability of porous medium. The hydraulic head, $h = z - \frac{p}{\rho g}$ relates z the height [m], p the pressure [Pa], ρ the density [kg/m^3] and g [m/s^2] the gravitational acceleration.

2.3.2 Single phase flow

Darcy's law for single phase fluids is as shown in Equation 7. It was derived from Navier-Stokes equation then modified by Hubbert who averaged it and neglected viscous and inertial effects and lastly modified by Whitaker. P is the pressure of the fluid and z refers to the vertical coordinate (Lie, 2019).

$$\vec{v} = -\frac{k}{\mu}(\nabla p - g\rho\nabla z) \qquad \text{Equation 7}$$

On a macroscopic scale, single-phase flow can be modeled by making a continuum assumption. By applying the law of mass conservation stating that mass accumulating inside the volume equal the net flux over the boundaries, a continuity equation that demonstrates the macroscopic behavior of single-phase fluid can be shown in Equation 8. $\emptyset$ refers to rock porosity, v is Darcy macroscopic velocity, ρ is density and q is fluid source or sink (fluid outflow/inflow per volume) (Lie, 2019).

$$\frac{\partial(\emptyset\rho)}{\partial t} + \nabla.(\rho\vec{v}) = \rho q \qquad \text{Equation 8}$$

In the case of compressible flow, the fluid and rock compressibilities will be taken into account and Equation 8 can be rewritten into Equation 9 and substituting in Equation 7 for the term $\vec{v}$ (Lie, 2019).

$$c_t\emptyset\frac{\partial p}{\partial t} - \nabla.[\frac{\rho k}{\mu}\nabla(p - g\rho z)] = \rho q \qquad \text{Equation 9}$$

Where c_t is the total compressibility of the rock and fluid compressibilities, ρ and c_t depend on pressure. The relationship between porosity and compressibility is as shown in Equation 10. (Lie, 2019).

$$\emptyset(p) = \emptyset_o + c_t(p - p_{ref}).$$ Equation 10

In the case of incompressible flow, total compressibility will equal zero, and both density and porosity are independent of pressure, as demonstrated in Equation 11 (Lie, 2019).

$$-\nabla.[\frac{\mathrm{k}}{\mu}\nabla(p - g\rho z)] = q$$ Equation 11

2.3.3 Multiphase flow

For multiphase flow, in this research case we account for two phases water and oil. The continuity equation for each phase can be written as shown in Equation 12.

$$\frac{\partial(\emptyset P_w S_w)}{\partial t} + \nabla\rho_w q_w = \rho_w q_w$$
$$\frac{\partial(\emptyset P_o S_o)}{\partial t} + \nabla\rho_o q_o = \rho_o q_o$$ Equation 12

The term $\frac{\partial(\emptyset P_w S_w)}{\partial t}$ is defined as the accumulation term, while $\nabla\rho_w q_w$ is the transport term. The term S refers to saturation, w refers to water and o refers to oil. The terms porosity $\emptyset$ and permeability depend on rock properties, while densityρ, pressure P and viscosity depend on the phase.

The application of Darcy's Law on the two phases can be as shown in Equation 13, where k is absolute permeability and k_{rw} is relative permeability for water phase.

$$q_w = \frac{-k}{\mu_w} k_{rw}(\nabla P_w - \rho_w g \nabla z)$$
$$q_o = \frac{-k}{\mu_o} k_{ro}(\nabla P_o - \rho_o g \nabla z)$$ Equation 13

3. METHODOLOGY

3.1 Reservoir Simulator

Reservoir simulators can be used to model reservoirs to predict the performance of the fluids over time and evaluate the reservoir production under potential scenarios, such as injecting various fluids. The reservoir modelled includes petro-physical characteristics that can be adjusted to understand the behavior of the fluids in the reservoir under specific conditions (Firozjaii et al., 2019).

The simulator needs to be calibrated, also known as history matched, where a historical pressure and production data from real reservoirs are used as the modelling parameters. This will allow the simulation to compare realistic models and examine the performance of the oil recovery methods being investigated to reach accurate conclusions. Some of the parameters that can be adjusted to control polymer flooding include polymer concentration, viscosity, reservoir porosity, salinity and reservoir permeability (Firozjaii et al., 2019).

3.2 Reservoir Simulation Software

SINTEF Technology and Society, a Norwegian independent research organization, developed the Matlab Reservoir Simulation Toolbox, MRST. This program can be used to simulate and model reservoirs. MRST contains modules that provide tutorials on different topics including enhanced oil recovery. It allows the user to use various computational methods and vary any parameters (Lie, 2019).

The module called ‘ad-eor’ is utilized to simulate water flooding and polymer injection in multiphase and compressible flow (SINTEF, 2020). Parameters can be redefined to prototype

the reservoir that needs to be simulated, modifications can be done to the size of the reservoir, rock properties, density, viscosity, Corey correlation of relative permeability, pressure at the wells and more. Computational methods can be used to calculate saturations, pressures and the time it takes for the simulation to take place.

MRST will be the tool used in this research to evaluate the behavior of the fluids over time for water flooding and polymer flooding. Parameters will be adjusted to match ones from industrial applications. Other parameters will also need to be changed to entertain any limitations needed specifically for a polymer such as HPAM to be used. The effect of some of the reservoir characteristics will be tested, such as the porosity and permeability. To measure how those parameters, affect the oil production, saturations of oil and water, pressure difference along the reservoir will be measured.

The effect of shear effect on the sweep efficiency in polymer flooding will also be evaluated using the module of 'blackoilpolymer'. This module will allow for different phases to flow without mixing; hence it will test the condition of a heterogeneous reservoir. For this project, two phase flow is considered, where water (or polymer) and oil will flow at the same time to evaluate the how much oil is being displaced by the injected fluid.

4. SIMULATION RESULTS AND DISCUSSION

4.1 One-Dimensional Homogeneous Simulation (Polymer Flooding Vs. Water Flooding)

For this simulation, a one-dimensional Cartesian grid of 100 m in length and 1 m width and 1 m height was modelled. The oil viscosity is 2 cP and its density is 0.9 kg/L. The power used in the Corey correlation of the relative permeability is 2. The rock porosity is 20% and permeability is 100 mD.

The aim for this model is to compare the water injection with the polymer injection in a simulation that mimics a sandstone reservoir at 50°C. The primary purpose of adding polymer to water to carry out polymer flooding is to increase the viscosity of the water flood. For this simulation, an assumption is made that the polymer solution rheology was Newtonian, so for polymer injection a thicker viscosity than the water's is used. Water injection has a viscosity of 1 cP. For the polymer injection, viscosities of 7 cP, 16 cP and 28 cP are tested.

The concept of reduced saturation is used in this simulation, so water and oil saturations will vary between 0 and 1.

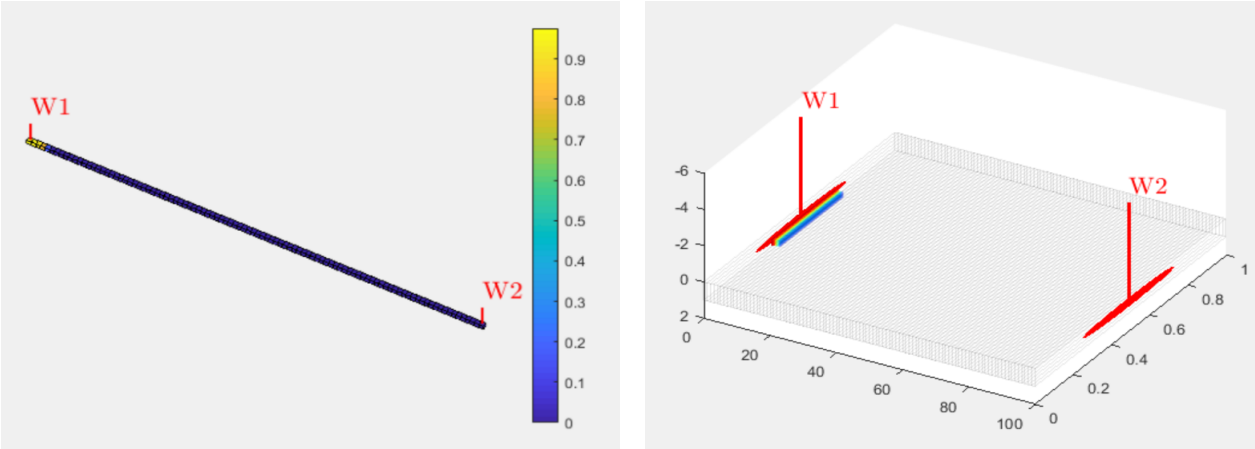

Figure 7: Reservoir Simulation for a one-dimensional reservoir of 100m length, 1m width, 1m height. W1 is injection well, W2 is production well

4.1.1 Reduced Oil Saturation Results

As demonstrated in the plot in Figure 8, the reduced oil saturation is 0 at the injection well eventually reaching saturation of 1 at the production well. For the water injection with a viscosity of 1 cP, the reduced oil saturation reached 0.5 around 40m into the reservoir. As the viscosity is increased to represent polymer injection, the oil saturation reaches total saturation at a shorter distance into the reservoir, the 28 cP injected fluid reached total saturation of 1 before reaching 20m into the reservoir. The reduced oil saturation had a greater increase earlier into the reservoir for the higher viscosity fluids as more oil was getting displaced by a more viscous fluid.

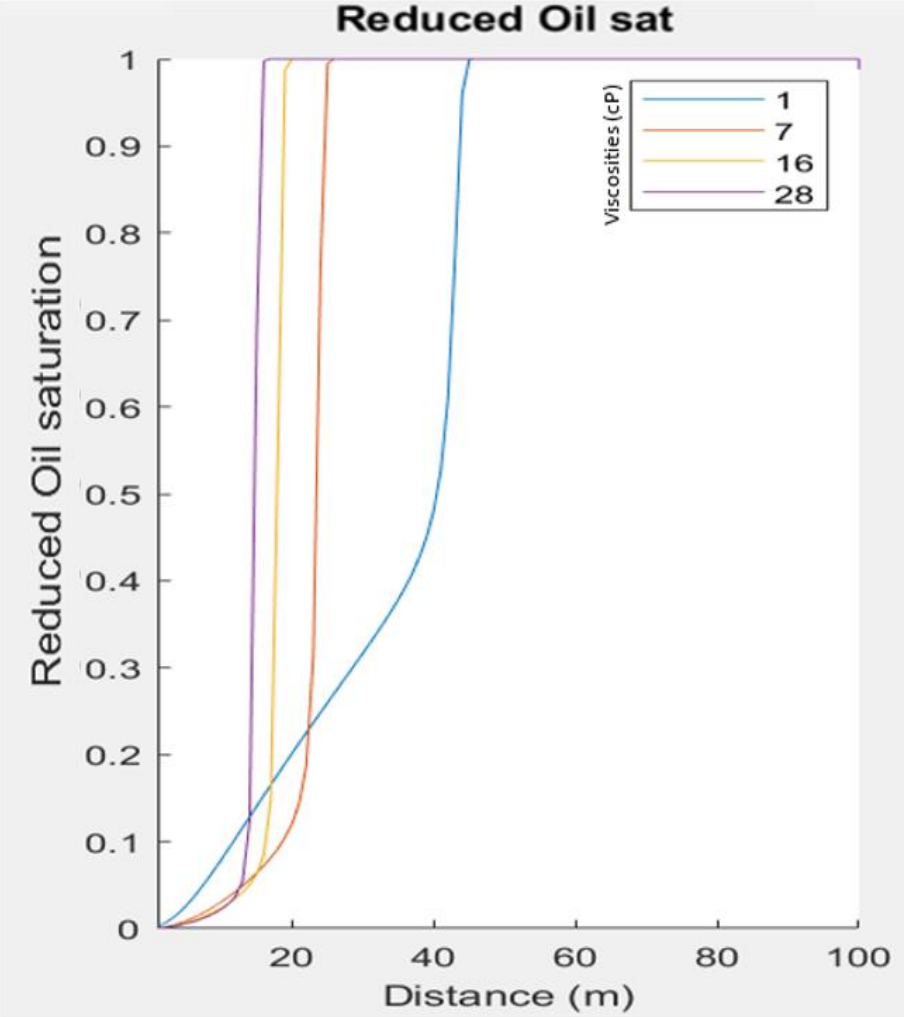

Figure 8: Reduced oil saturation results

4.1.2 Reduced Water Saturation Results

The plot in Figure 9 shows how the reduced water saturation starts at saturation of 1 at the injection well and eventually reached a saturation of 0 before even reaching the production well at 100m. For the water injection with a viscosity of 1 cP, the reduced water saturation reached 0.5 around 45m into the reservoir. As the viscosity is increased, the reduced water saturation reaches 0 at a shorter distance into the reservoir; the injected fluid with viscosity of 28 cP reached saturation of 0 at around 17m into the reservoir. The water is getting used up

more at a shorter distance into the reservoir for the higher viscosity fluids as it is displacing more oil.

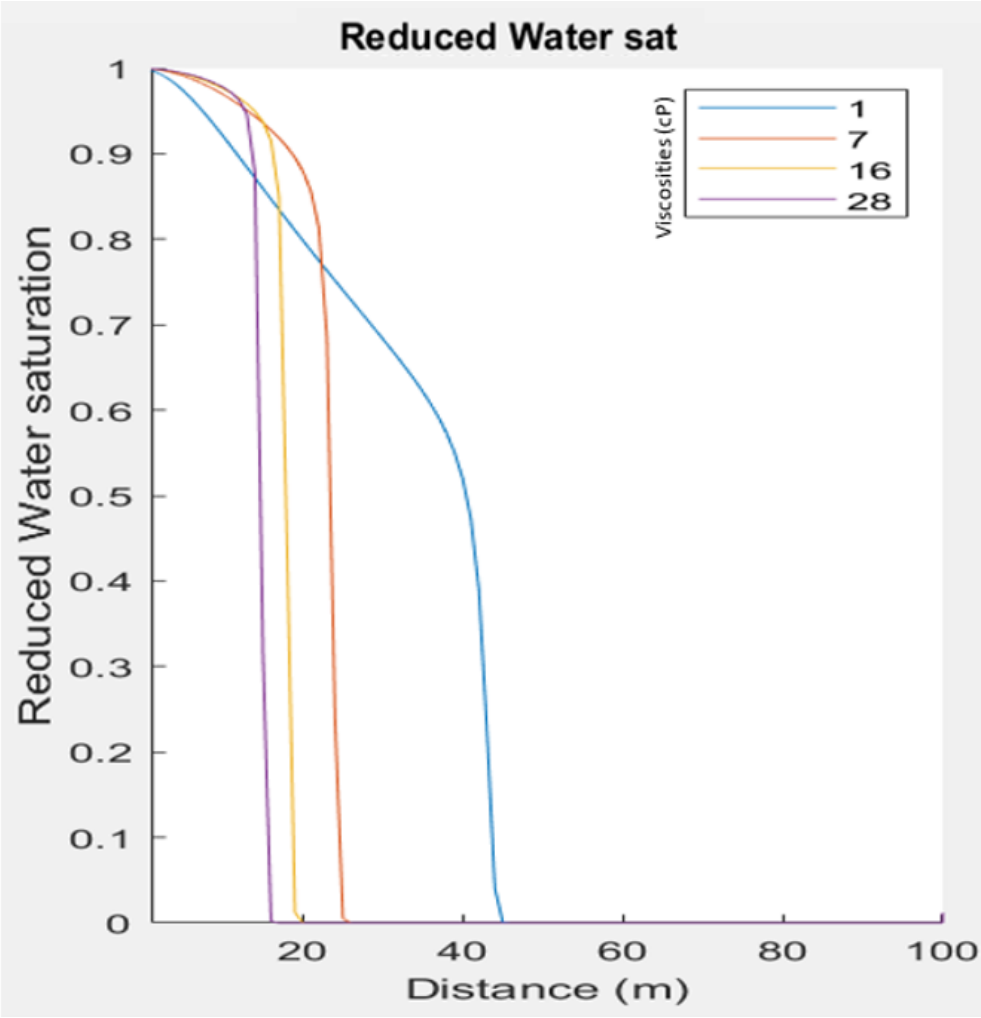

Figure 9: Reduced water saturation results

4.1.3 Pressure Change Results

The plot in Figure 10 shows how the pressure decreases along the reservoir from a starting pressure of 10^5 Pa at the injection well to 0 Pa at the production well at 100m. For the water

injection with a viscosity of 1 cP, the pressure dropped at the slowest rate across the reservoir. It reached a pressure of $2x10^4$ Pa at around 85m into the reservoir. As the viscosity is increased, the pressure drop was at a faster rate across the reservoir. The fluid injection with a viscosity of 28 cP reached a pressure of $2x10^4$ Pa at around 20m into the reservoir. The pressure drop is greater at a shorter distance for the higher viscosity fluids as more oil is being displaced. In a porous medium, fluid flows in the direction of decreasing pressure, thus pressure near the production well is lower. Pressure drops to attain equilibrium as oil gets produced, and a volume of water replaces its place. It can be seen that the pressure initially decreases at a fast rate until a certain distance into the reservoir where the pressure decrease gets slower. That turning point correlates with the reduced oil saturation change, where the reduced oil saturation becomes its highest value as most of it got displaced. For instance for the 28cP viscosity the turning point was at around 20m into the reservoir where the oil saturation as shown in Figure 8 has become 1.

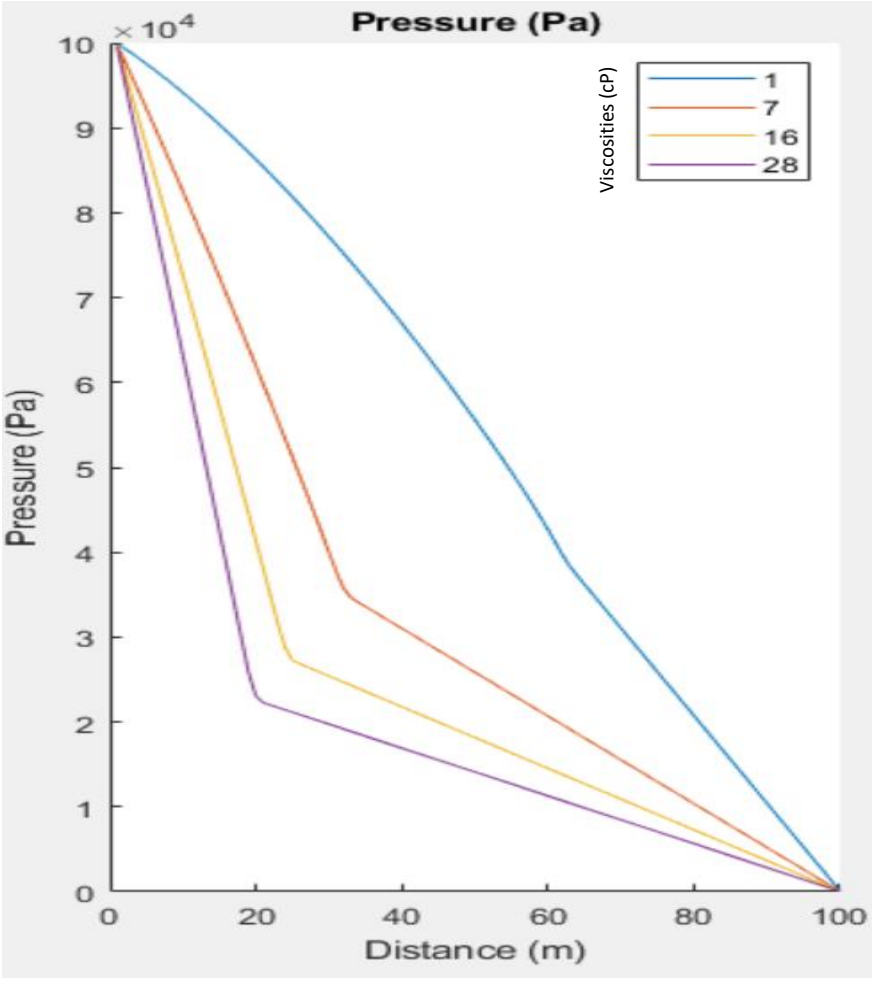

Figure 10: Pressure change results

4.2 Two-Dimensional Homogeneous Simulation (Polymer Flooding Vs. Water Flooding)

A two-dimensional simulation of a sandstone reservoir at 50°C was modelled with 150 m in length, 150 m height and 1 m width. The rock porosity is 20% and its permeability is 100 mD. The oil viscosity is 2 cP and its density is 900 kg/m^3. The power used in the Corey correlation of the relative permeability is 2. The simulation operated for 2 years. The pressure at the injecting well is 115 bar and the pressure at the production well is 85 bar. For this simulation, three viscosities of the injected fluid were compared, 1 cP for water injection, 7 cP

and 15 cP for polymer injection. The actual dimension target is 1500m length, 1500m height, and 10m width which was discretized into 150m x150m x1m Cartesian grid cells. As for time, the simulation target run is for 2 years accounting 7 days a week.

4.2.1 Reduced Oil Saturation Results

Demonstrated in Figure 11 is the evolution results for reduced oil saturation versus time at a specific location in the reservoir that is 30 m into the height and 30 m into the length, cell [30, 30]. The oil saturation at that location decreases over time as it gets displaced. The more viscous fluids took longer time to start displacing the oil as they flow slower, however, they displace more oil at the end. By the end of the operation time, the injected fluid with the highest viscosity value of 15 cP reached an oil saturation of 0.048, while, the fluid with viscosity of 7 cP reached saturation of 0.056 and the water flooding with 1 cP reached a saturation of 0.123. Thus, the higher the viscosity of the injected fluid, the more oil gets displaced eventually.

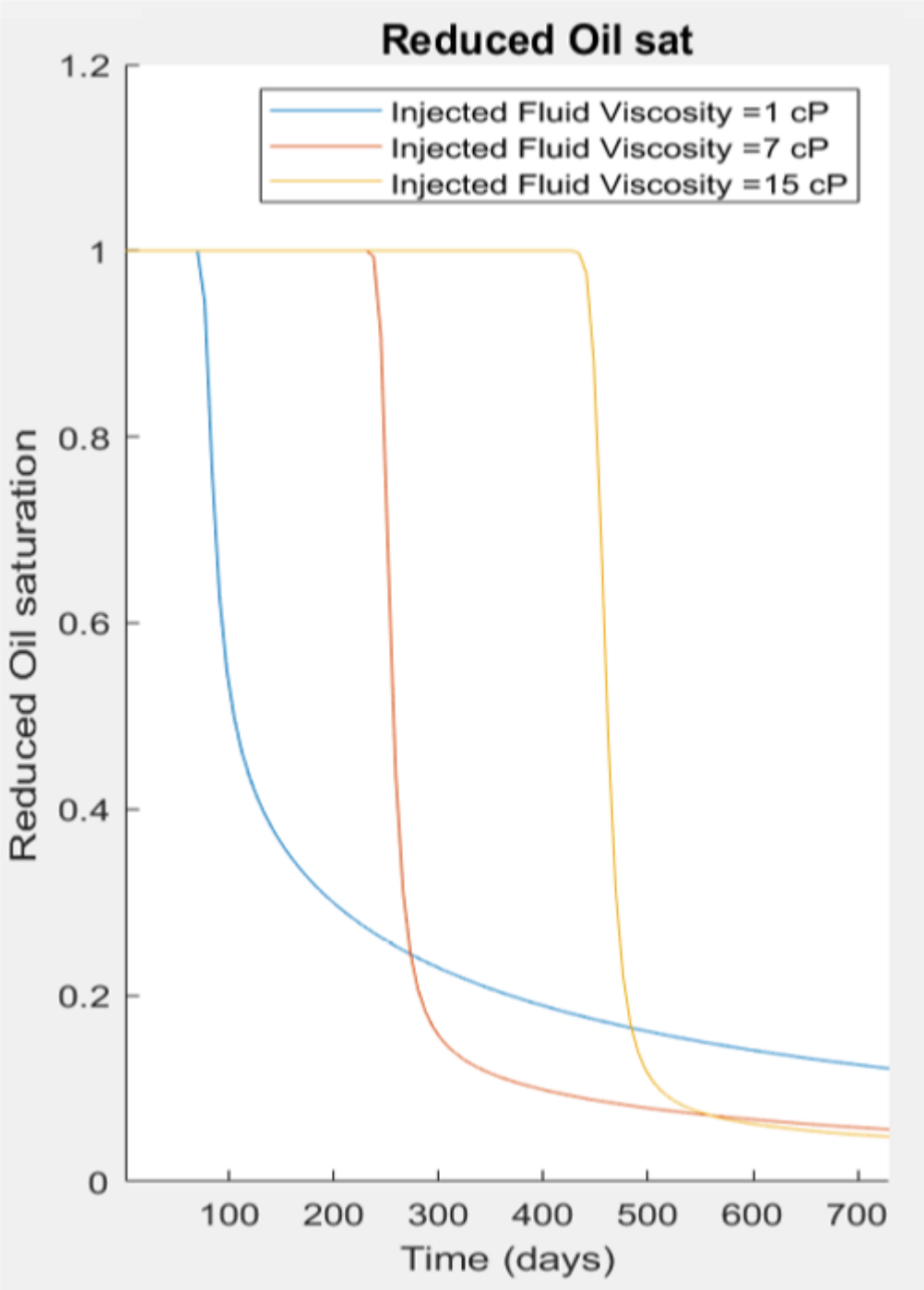

Figure 11: Reduced oil saturation results vs. time in cell [30,30]

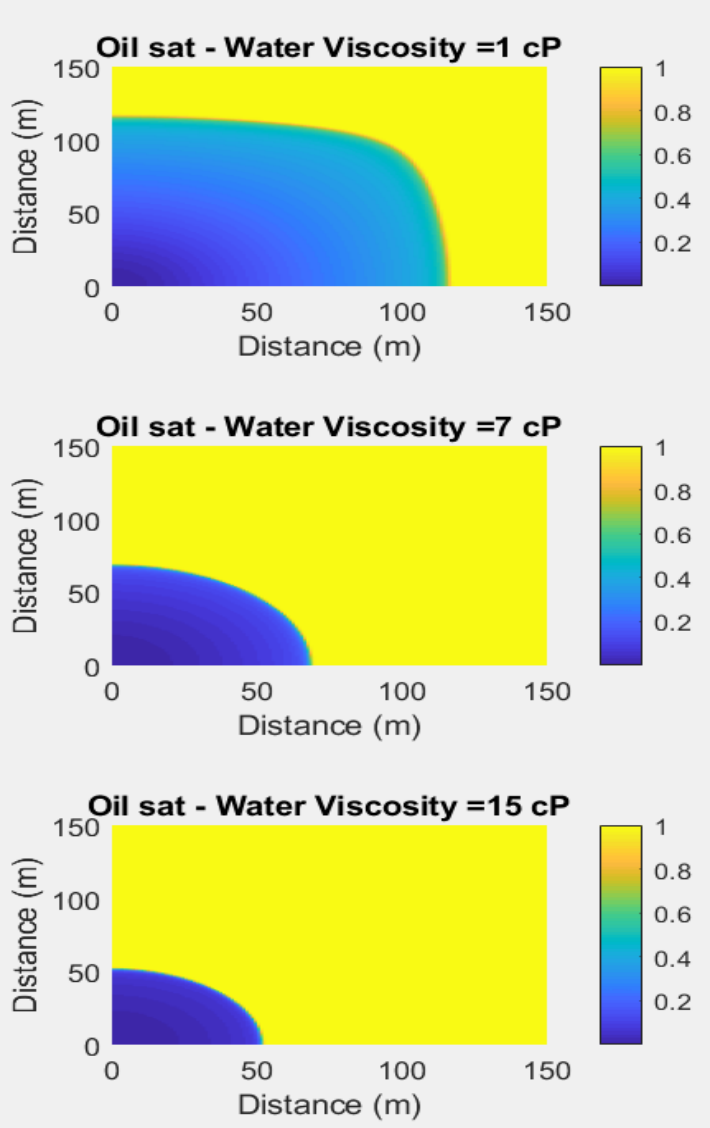

Figure 12: Reduced oil saturation results across the reservoir for each viscosity

Figure 12 shows the reduced oil saturation results across the reservoir for each viscosity as oil gets displace and its saturation decreases. The more viscous fluid takes longer time to displace oil, therefore the higher viscosity plots show less oil displacement at the moment this was captured. The 15 cP fluid had a 0.2 oil saturation at 50m into the height and 50m into the length, while the fluid with viscosity of 7 cP had a 0.2 oil saturation around 70m into both height and length.

4.2.2 Reduced Water Saturation Results

Shown in Figure 13 is the evolution of the reduced water saturation versus time at cell [30m, 30m] into the reservoir. The reduced water saturation at that location increases over time as it is continuously injected. The more viscous fluids take longer time at the start to start increasing in saturation, for instance the 7 cP fluid started increasing after 200 days, while the 15 cP started increasing after 400 days. Once they begin to increase in saturation, the process gets faster. It can be deducted that the more viscous the fluid the higher saturation it will reach eventually. Water injection with 1 cP reached a saturation value of 0.87, while, the polymer injection of 15 cP reached a saturation of 0.96 and the injected fluid of 7 cP reached a saturation of 0.94. The more viscous fluid eventually reached a higher saturation at that location meaning more oil was displaced.

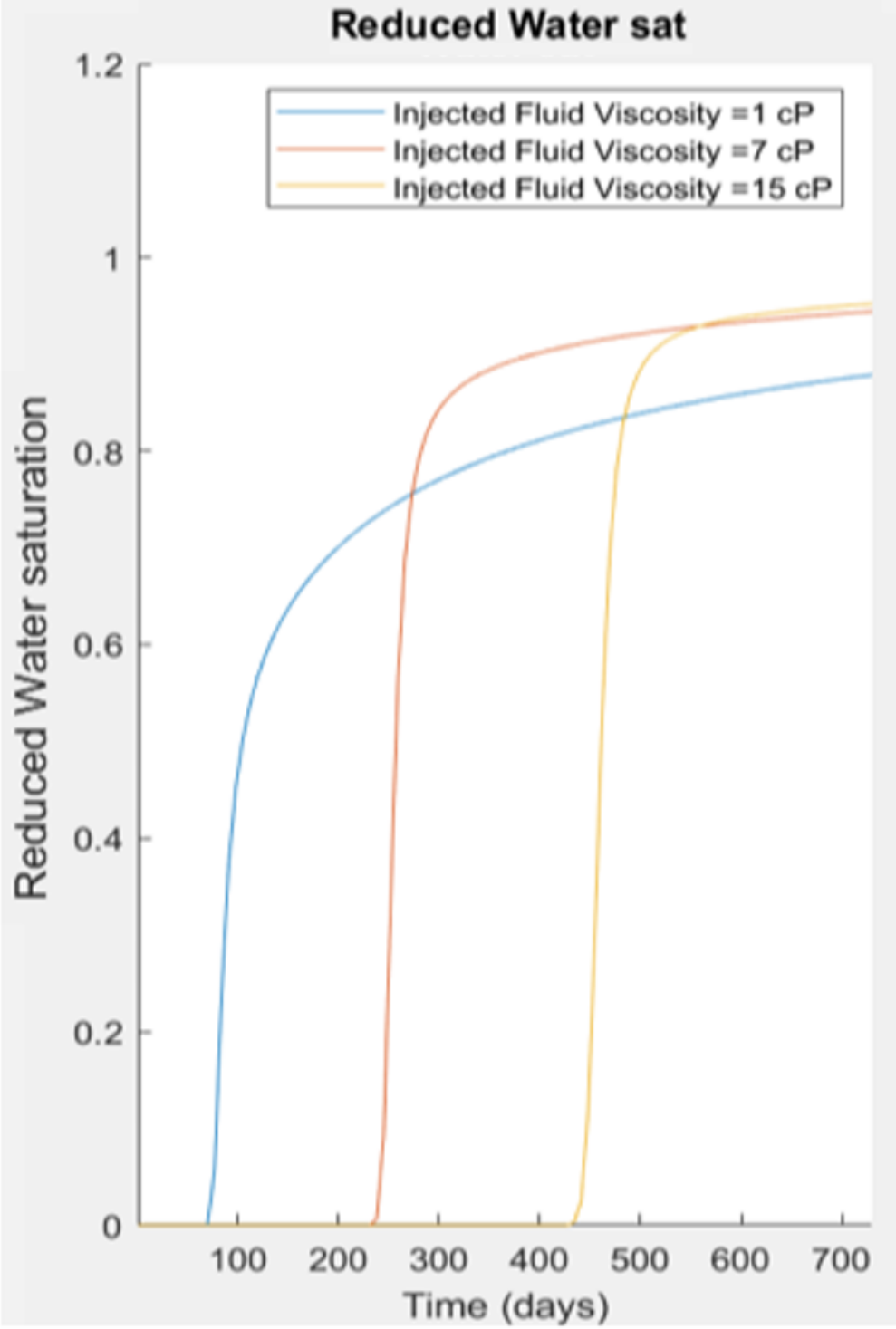

Figure 13: Reduced water saturation vs time in cell [30, 30]

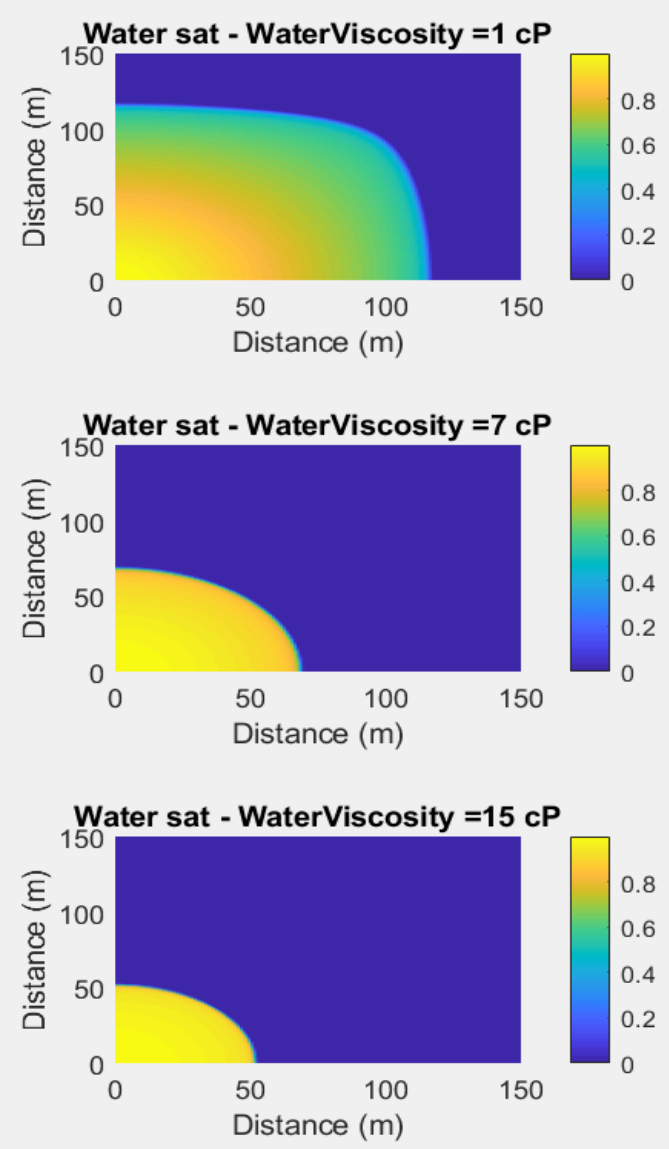

Figure 14: Reduced water saturation results across the reservoir for each viscosity

Figure 14 shows the reduced water saturation results across the reservoir for each viscosity as it gets injected into the reservoir. As shown for 15 cP fluid, since it is more viscous the saturation remains high about 0.9, 50m into the height and 50m into the length, while the fluid with viscosity of 7 cP reached 0.8 saturation around 70m into both height and length. The water injection with 1

cP flows the fastest when injected as seen by how the water saturation is almost 0.4 around 110m into the height and length.

4.2.3 Pressure Change Results

Figure 15 shows the pressure change versus time at cell [30m, 30m] into the reservoir. The pressure at the injection well is 115 bar and the pressure at the production well is 85 bar. The pressure decreases over time in the reservoir as oil gets produced. The water injection with 1 cP reached a pressure ranging between 107 and 103 bar over the simulation time in that location. The polymer injection of 15 cP had a pressure range between 92 and 90, while the injected fluid of 7 cP had a pressure ranging between 96 and 95. This shows how the more viscous fluid had lower pressure in that location, as more pressure decreased before the other fluids indicating more oil got produced.

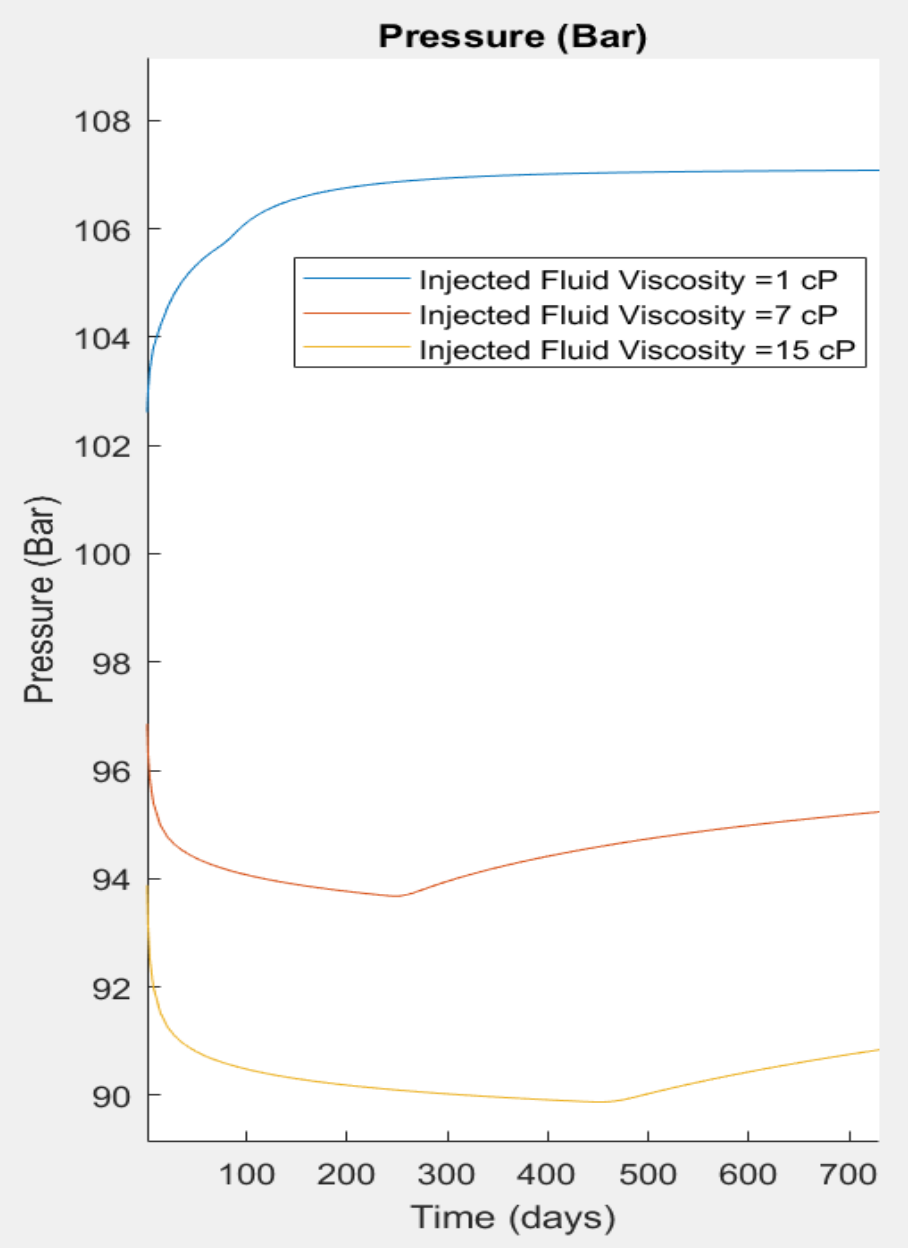

Figure 15: Pressure change results vs. Time in cell [30,30]

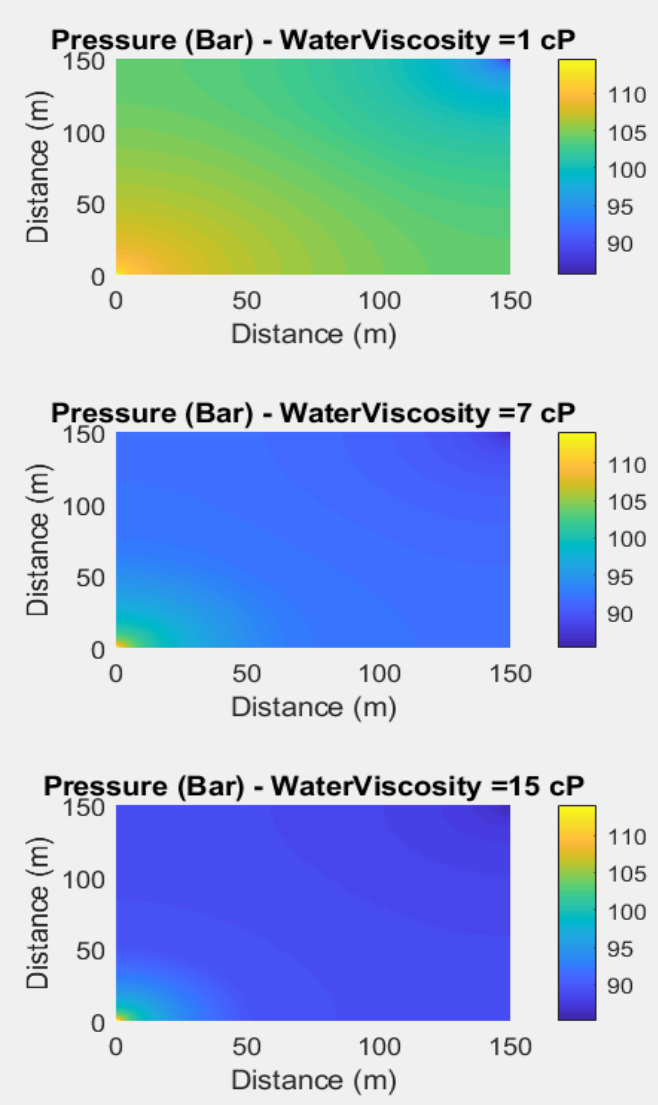

Figure 16: Pressure change results across the reservoir for each viscosity

As shown in Figure 16, pressure changes from 115 to 85 bar along the reservoir. For the water injection with 1 cP, the pressure took the longest time to decrease and reached around 95 bar at the very end of the reservoir at around 150 m. As for the polymer injection with 15 cP, the pressure decreased the fastest and reached 85 bar around 50 m into the reservoir. The polymer injection with 7 cP also had a fast pressure decrease but was still slower than the 15 cP fluid

4.3.Three-Dimensional Homogeneous Simulation (Polymer Flooding Vs. Water Flooding)

The following is an adjoint simulation that illustrates water and polymer flooding in a 3D homogeneous reservoir, using the 'adjointWithPolymerExample' module in the MRST software (SINTEF, 2020). The Cartesian grid is 31 by 31 by 3 grid cells to represent a simple box shaped reservoir. The production well is located in the center of the reservoir and two injection wells are located in the northeast and southwest corners as shown in Figure 18 below. Two cases are simulated, one being polymer flooding followed by water flooding and another being pure water flooding. The operation duration is 7 years, where polymer gets injected three years into operation time for the case of polymer flooding.

4.3.1 Production Plot For Polymer Flooding vs Water Flooding

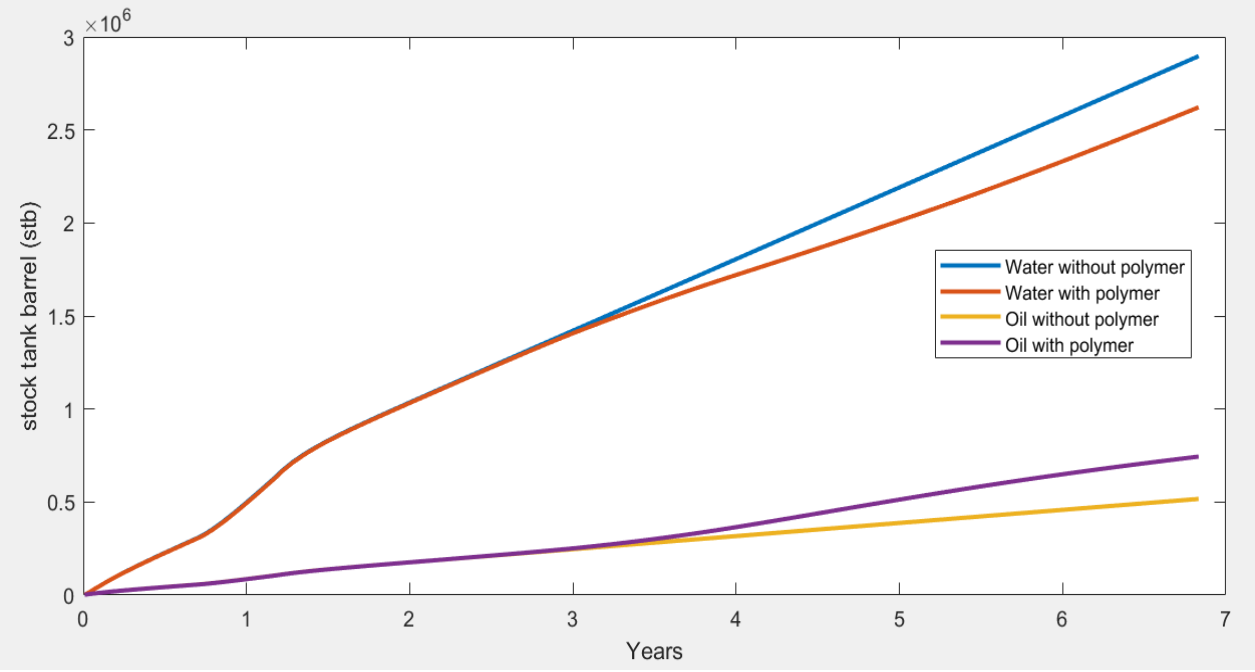

Figure 17: Water and Oil Production for Water flooding and Polymer flooding (From MRST)

As shown in Figure 17, the plot shows the accumulated water and oil production for both cases of polymer flooding and pure water flooding. The polymer injection gives more oil production and less water production compared to pure water flooding; hence polymer flooding enhances oil recovery more than water flooding.

4.3.2 Injection Results over Time

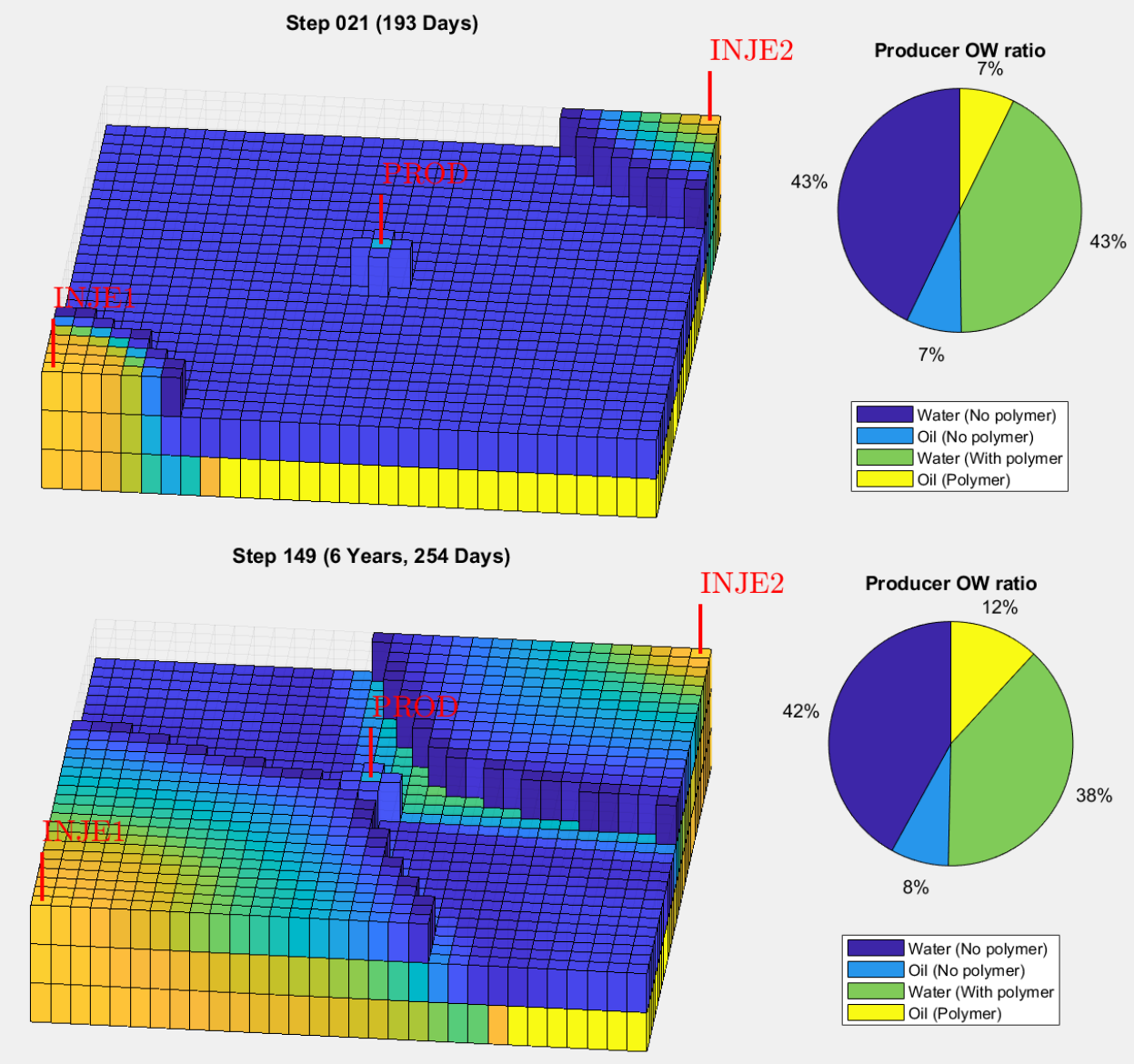

Figure 18: Process of water flooding and polymer flooding (From MRST)

Figure 18 shows how the injection wells were located at the corners, with the production well located in the center. The Cartesian grid shows the change of oil and water saturation over the years of operation. The top picture shows progress at 192 days and the bottom one shows progress after 6 years and 254 days. The pie chart shows oil to water ratio in the producer well for both cases with and without polymer. Comparing the top and bottom charts, it can be deduced that oil ratio has increased for both cases, but more noticeably for the case with polymer injection. This indicates more oil was being produced in the polymer flooding case.

4.4.Black Oil Polymer Simulation (With Vs. Without Shear Effect)

The model 'blackoilpolymerTutorial2D' from the module 'ad-eor' in the MRST software is used to simulate polymer flow in a 2D heterogeneous reservoir (SINTEF, 2020). In the black oil model, phases do not mix. Two phases are being simulated in this simulation, water/polymer and oil. According to Bao (2017), in the black oil model the distinction between the two phases depends on their characteristics such as their viscosity to determine which fluid will displace the other. In this case, the polymer increases the viscosity of the aqueous phase that transports it.

Table 1: Defined Parameter Values of Reservoir Conditions

Defined Parameters	**Values**		
Reservoir Geometry	4000m x 200m x 150m		
	Discretized into: 20m x 5m x 1m Cartesian grid cells		
Porous Media Characteristics	**Porosity**	0.3	
	Permeability	100 mD	
Fluid Characteristics	**Oil**	**Viscosity**	90 cP
		Density	0.9 kg/L
		Gravity	25 API
	Water	**Viscosity**	1 cP
		Density	1000 kg/m^3
	Polymer	**Viscosity**	15 cP
		Concentration	1000 ppm
Boundary Conditions	**Injection well** (located bottom 2 layers)	Injection rate: 1000 m^3/day	
		Bottom hole pressure: 450 bars	
	Production well (located top 2 layers)	Bottom hole pressure: 260 bars	
Duration	#1 Water flooding: 1260 days		
	#2 Polymer slug injection: 1700 days		
	#3 Water flooding resumes: 7990 days		
Phases	2 – Water or Polymer and Oil		

4.4.1. Injection Well Results

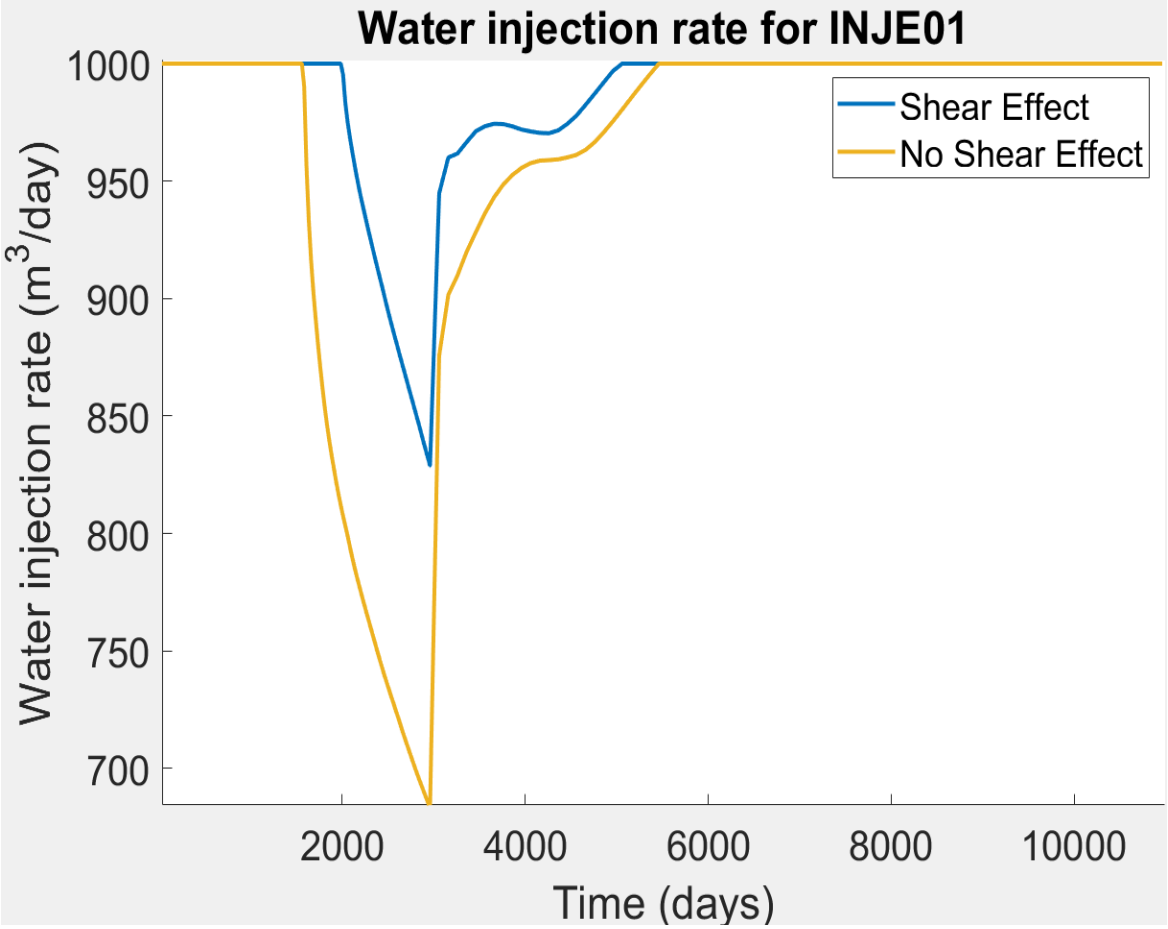

Figure 19: Water injection rate with and without shear effect (From MRST)

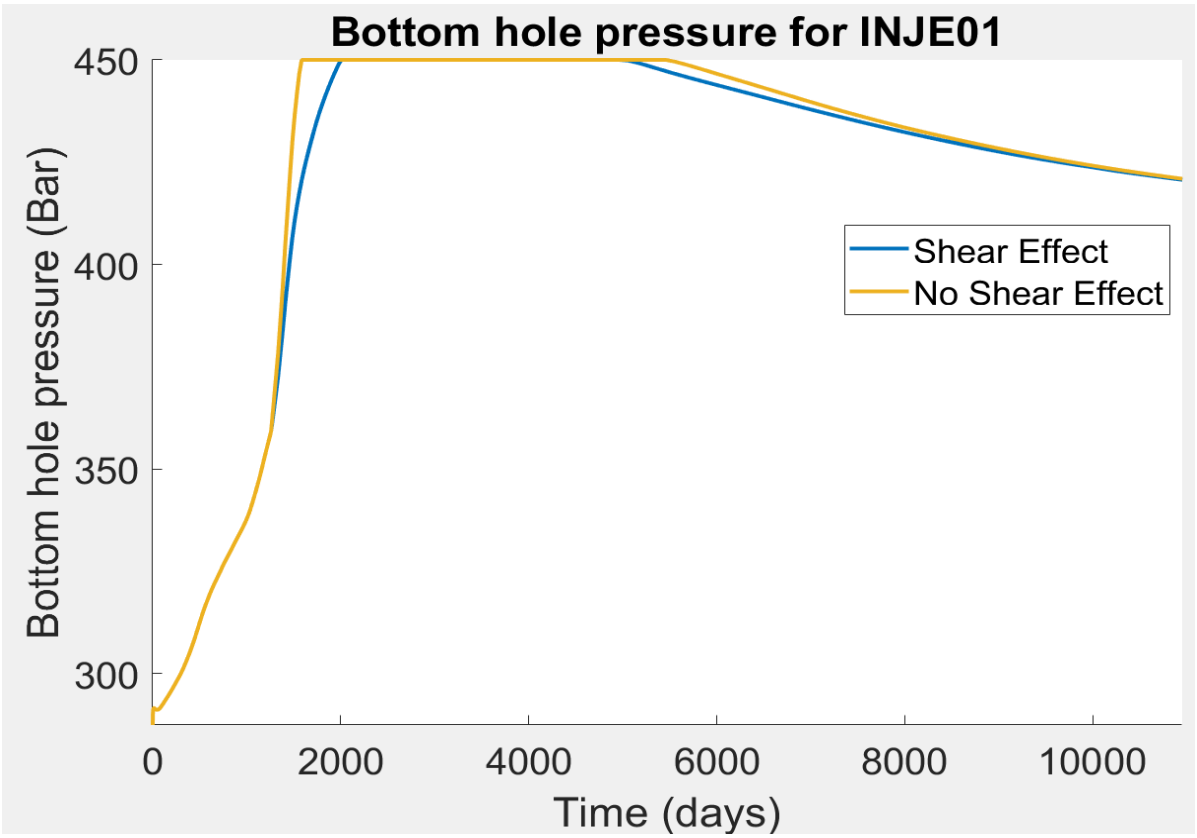

Figure 20: Bottom hole pressure in injection well with and without shear effect (From MRST)

Polymer flooding in this simulation starts with water injection for 1260 days, followed by polymer injection of 1000ppm HPAM for 1700 days then water injection resumes. The simulation accounts for 30 years operation. Looking simultaneously at Figures 19 and 20, the change in the water injection rate can be seen in accordance to the change in the bottom hole pressure. For the first 1000 days of pure water injection, it can be seen that the pressure is slowly increasing and the water injection rate remains constant at 1000m^3/day. As the polymer starts to get injected after 1260 days, it can be seen that the bottom hole pressure begins to increase faster until it reaches the

upper limit of 450 bars. The polymer injected was increasing the viscosity of the water injected and lowering its mobility, hence decreasing the rate at which it is injected. Higher bottom hole pressure could have helped maintain the injection rate, but the upper limit has already been reached. After 1700 days of polymer injection, the pure water injection resumes and the injection rate increases back to 1000m^3/day for the remaining days of operation. From Figure 19, it can be seen that shear thinning behavior had better injectivity as it didn't decrease the injection rate as drastically as the one without shear effect, hence more oil was displaced when shear effect is considered.

4.4.2 Production Well Results

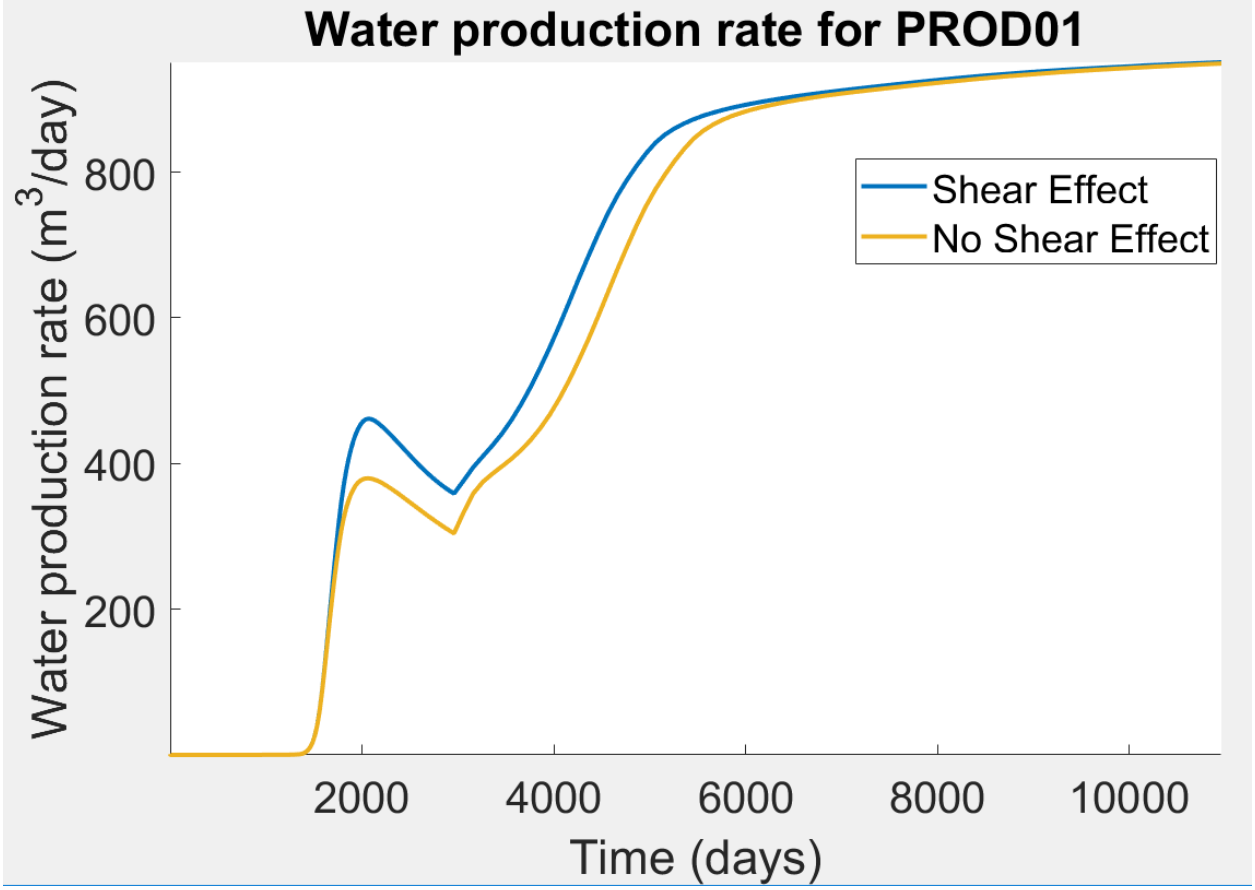

Figure 21: Water production rate with and without shear effect (From MRST)

It was shown in Figure 19 that the case with shear effect had higher water injection rate, which is again shown in Figure 21 as water production rate is higher for the case with shear effect. Once polymer was injected around 2000 days of operation water production rate slowed down and even started decreasing for some time corresponding to the decrease in water injection rate around the same time.

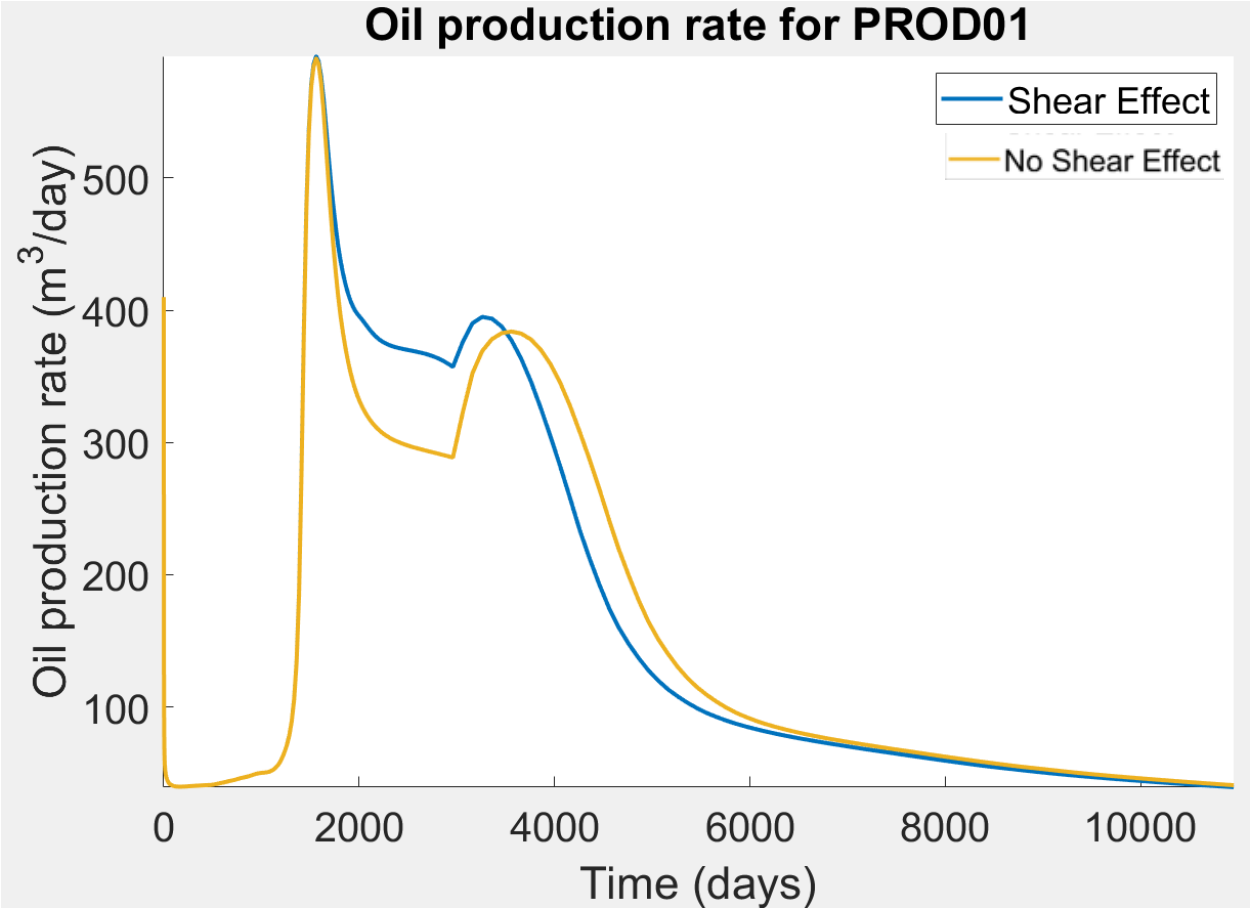

Figure 22: Oil production rate with and without shear effect (From MRST)

Figure 22 illustrates both cases of polymer flooding with and without shear effect have similar pattern overall. The case with shear effect had higher oil production rate around 2000 to 3750 days than the case without shear effect, then they switch as both cases decrease slowly as the operation comes to an end.

4.5.Effect Of Reservoir Characteristics On Sweep Efficiency

4.5.1 Effect of Reservoir Porosity

A two-dimensional simulation of a sandstone reservoir at 50°C was modelled with 150 m in length, 150 m height and 1 m width. The actual dimension target is 1500m length, 1500m height, and 10m width which was discretized into 150m x150m x1m Cartesian grid cells. As for time, the simulation target run is for 2 years accounting 7 days a week. The rock permeability is 100 mD. The oil viscosity is 2 cP and its density is 900 kg/m^3. The power used in the Corey correlation of the relative permeability is 2. The pressure at the injecting well is 115 bar and the pressure at the production well is 85 bar. For this simulation, two porosities of the reservoir were compared, 20% and 40% for both a water flooding case with 1cP viscosity and 1000 kg/m^3 density and a polymer flooding case with 3 cP viscosity that is assumed to behave Newtonian.

4.5.1.1 Reduced Oil Saturation Results

Figure 23 shows how oil saturation in cell [30,30] decreases over time for each porosity. Porosity is defined as the void fraction over total bulk volume, it's the empty space between the rock grains that hold fluid within. Hence the bigger porosity means more fluid can be stored within and may take longer time to be emptied. Saturation describes the phase volume over the pore

volume, hence a small pore can't hold too much of that phase. As shown in the plot for the lower porosity oil saturation decreases faster since the smaller pores are not as filled as the bigger pores. It is similar for both water and polymer flooding, however polymer flooding is slower since a more viscous fluid is being injected and takes longer to displace the oil.

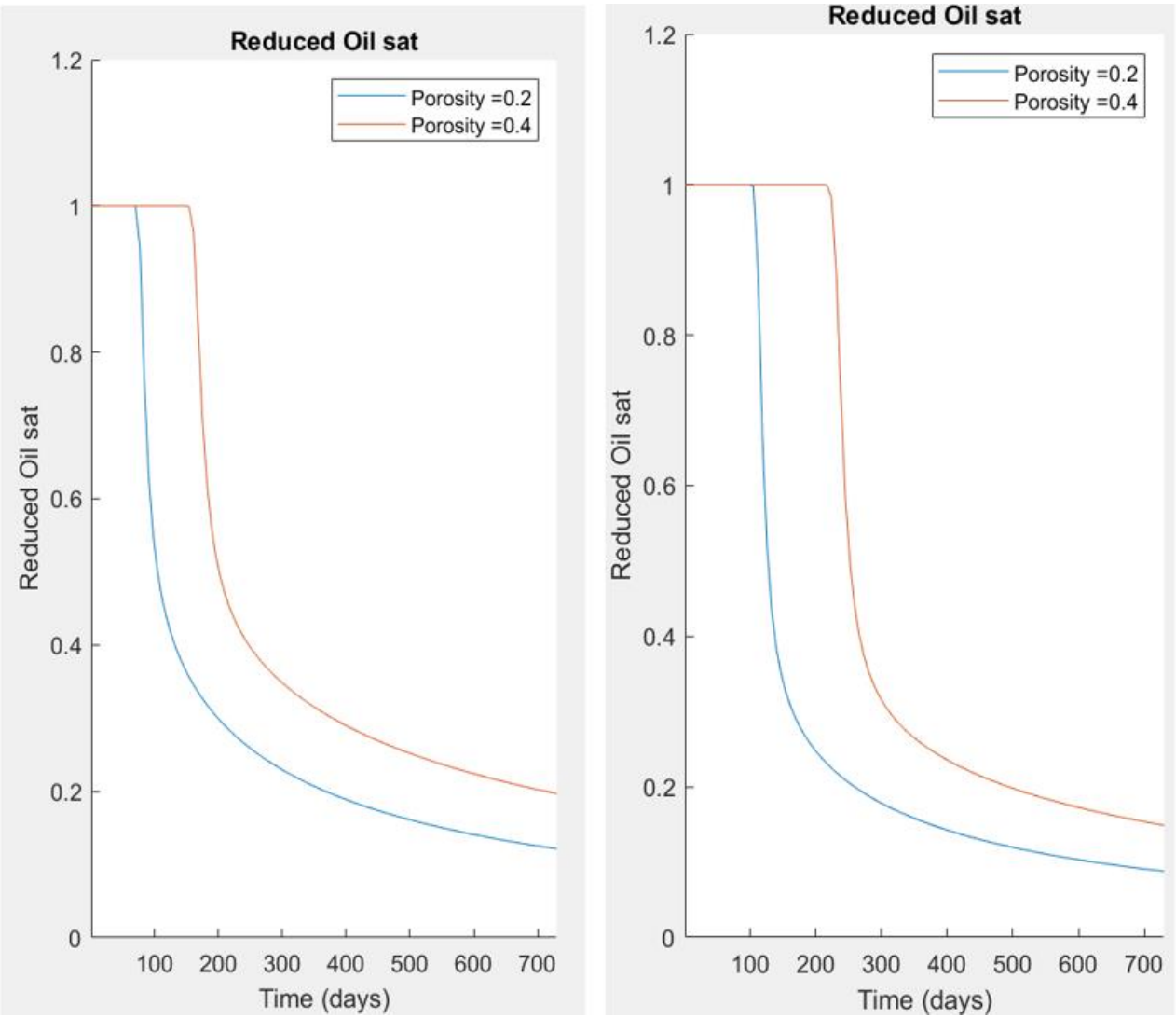

Figure 23: Reduced oil saturation results in cell [30,30] for water flooding (left) and polymer flooding (right) for each porosity

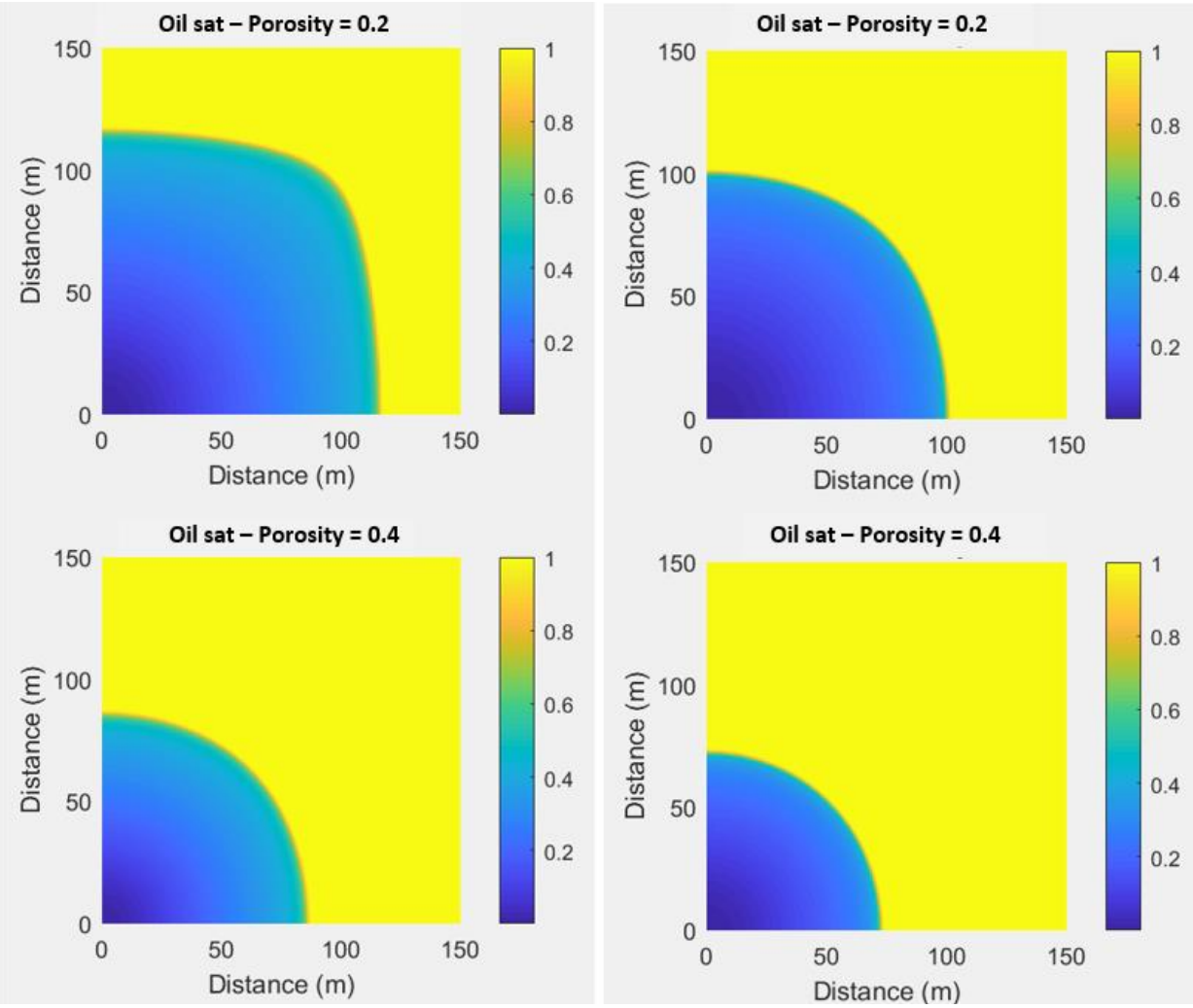

Figure 24: Reduced oil saturation results over distance for each porosity for water flood (left) and polymer flood (right)

Figure 24 illustrates how the reduced oil saturation decreases within the reservoir for each porosity. The injection well is located at [0, 0] and the production well is at [150,150]. It can be seen similar to what Figure 23 has shown that for the lower porosity the oil saturation was decreasing faster. For each porosity the oil saturation is relevant to that pore volume, the smaller pores may not be

as filled as the larger pores, which is shown by how the smaller the pores the faster it gets emptied of oil. The larger pores take longer time to drain out what's inside.

4.5.1.2 Reduced Water Saturation Results

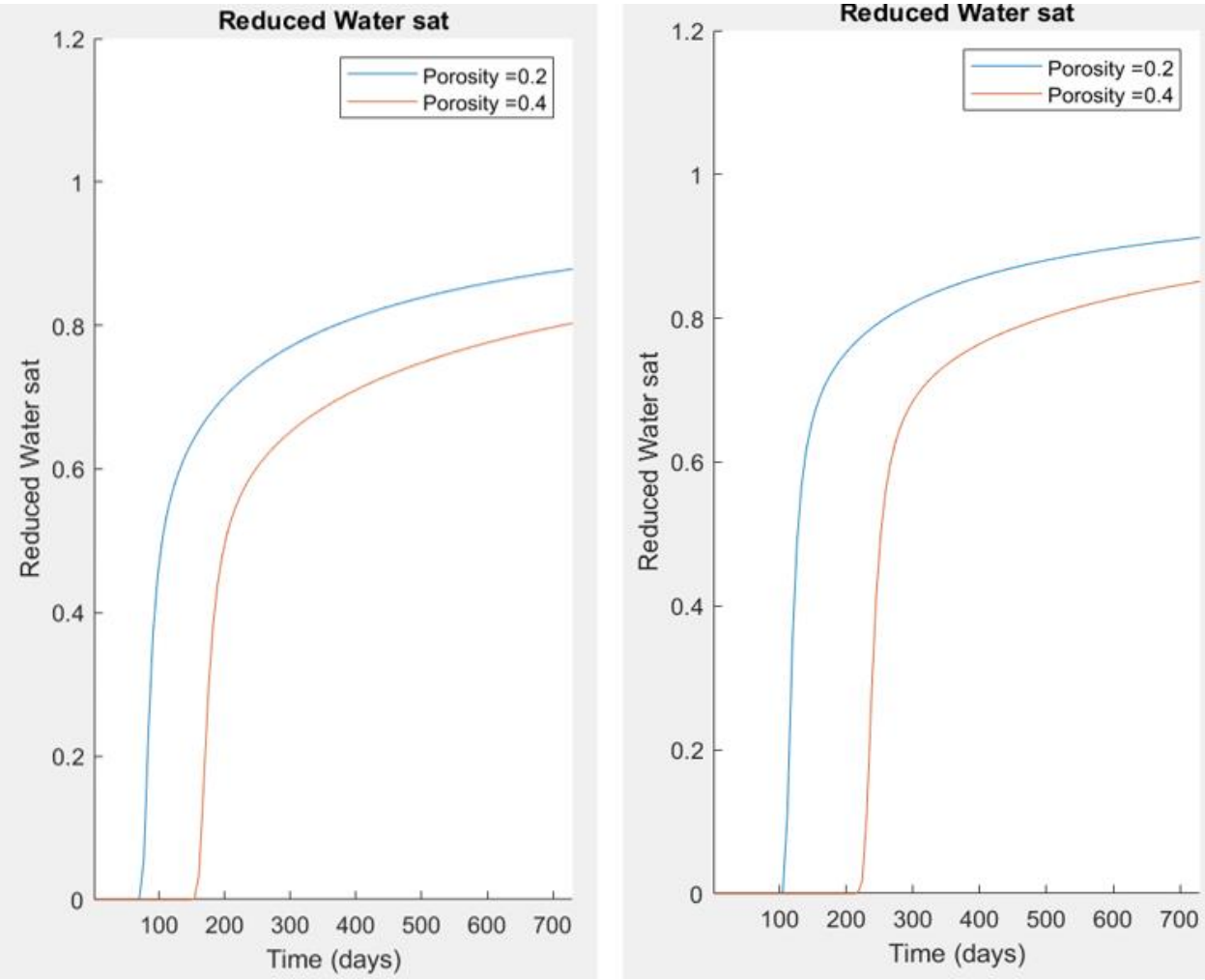

Figure 25: Reduced water saturation results in cell [30,30] for water flooding (left) and polymer flooding (right) for each porosity

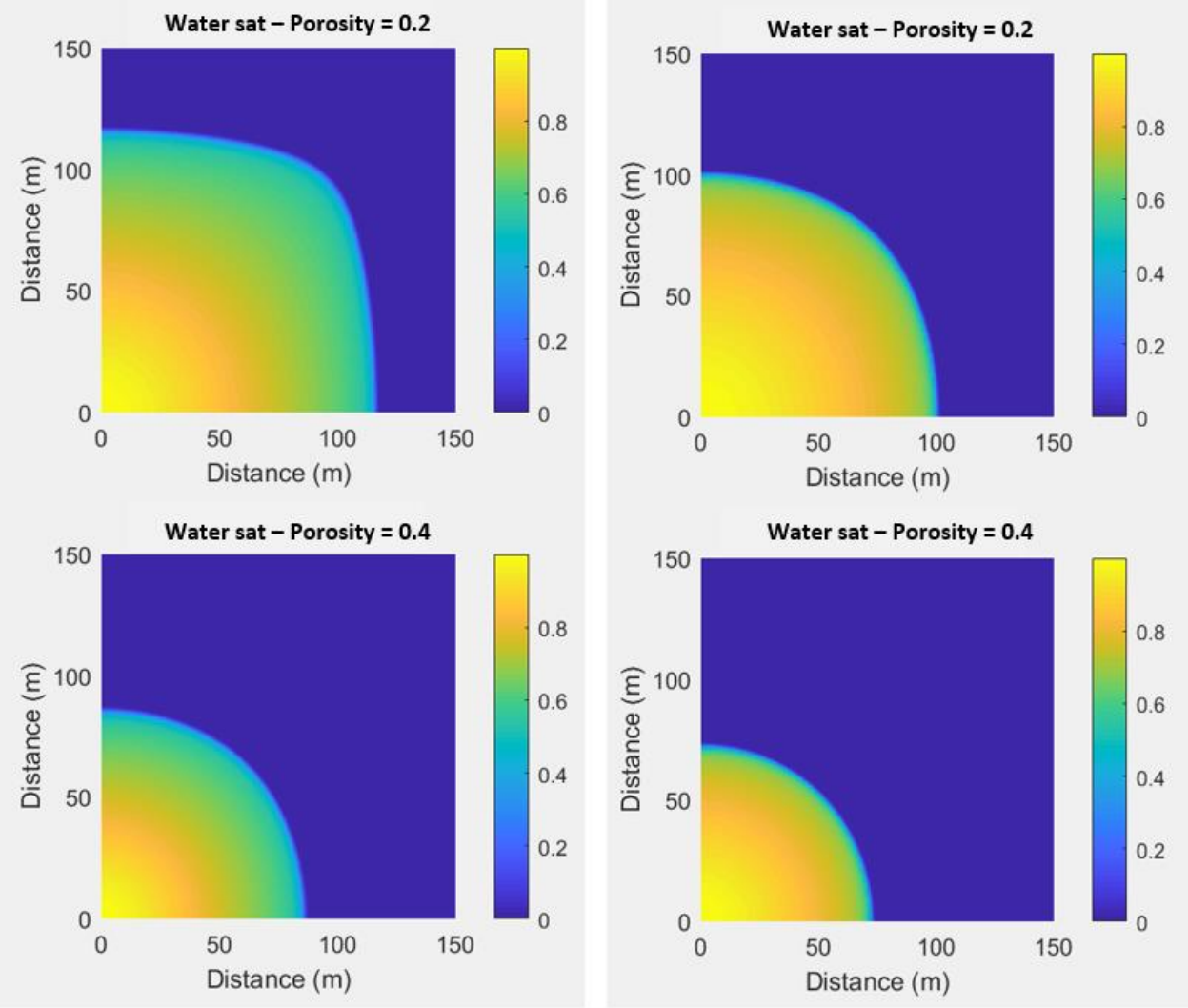

Figure 26: Reduced water saturation results over distance for each porosity for water flood (left) and polymer flood (right)

Figure 25 demonstrates the reduced water saturation change in one location over time and Figure 26 shows the reduced water saturation change over the distance within the reservoir. Both agreeably show how the lower porosity had faster water saturation increase as the void space is smaller and quickly fills up with the water being injected. Polymer flooding demonstrates a similar increase on a slower pace for being more viscous hence flows sluggishly as compared to just water flow.

4.5.1.3 Pressure Change Results

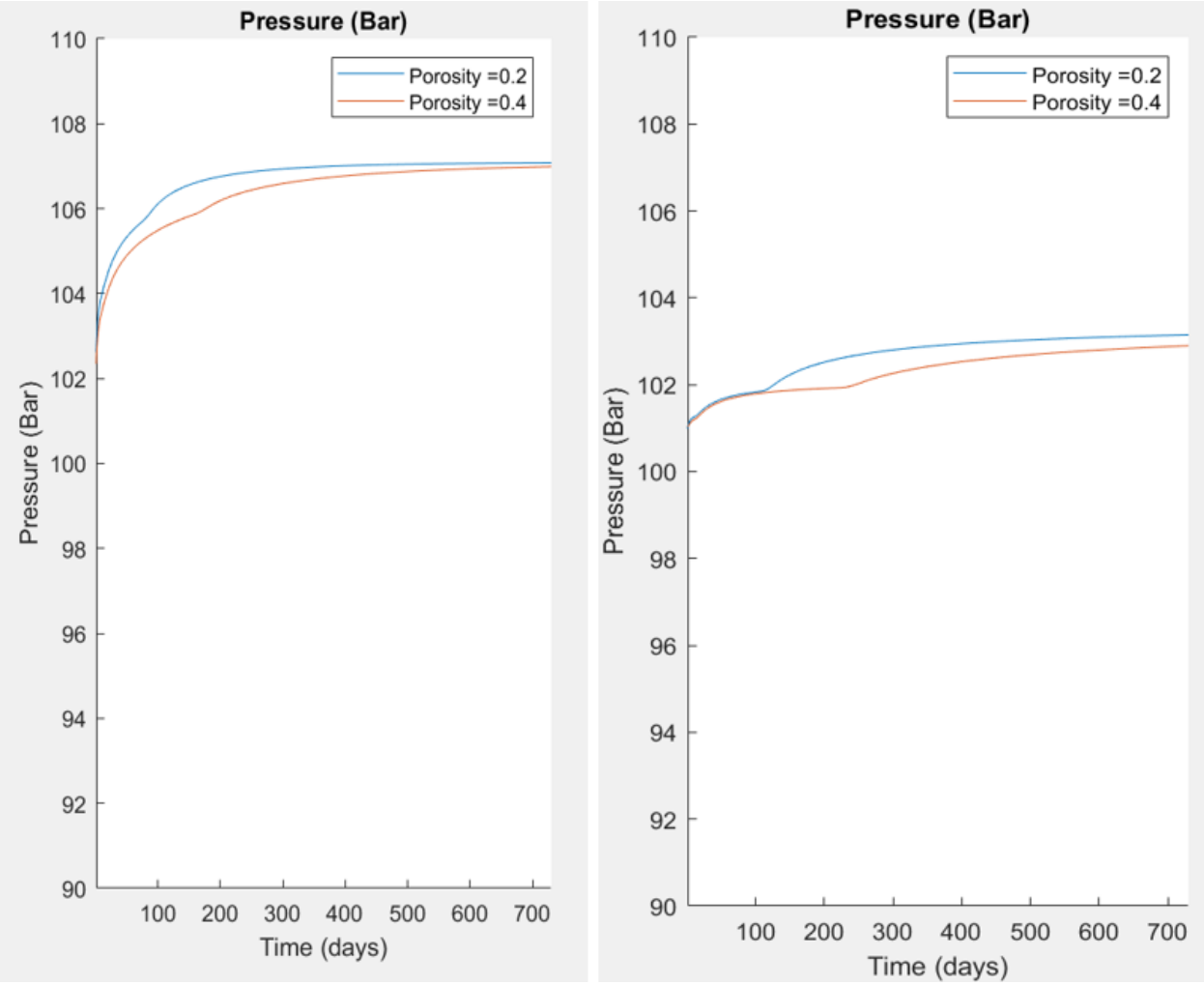

Figure 27: Pressure change results in cell [30,30] for water flooding (left) and polymer flooding (right) for each porosity

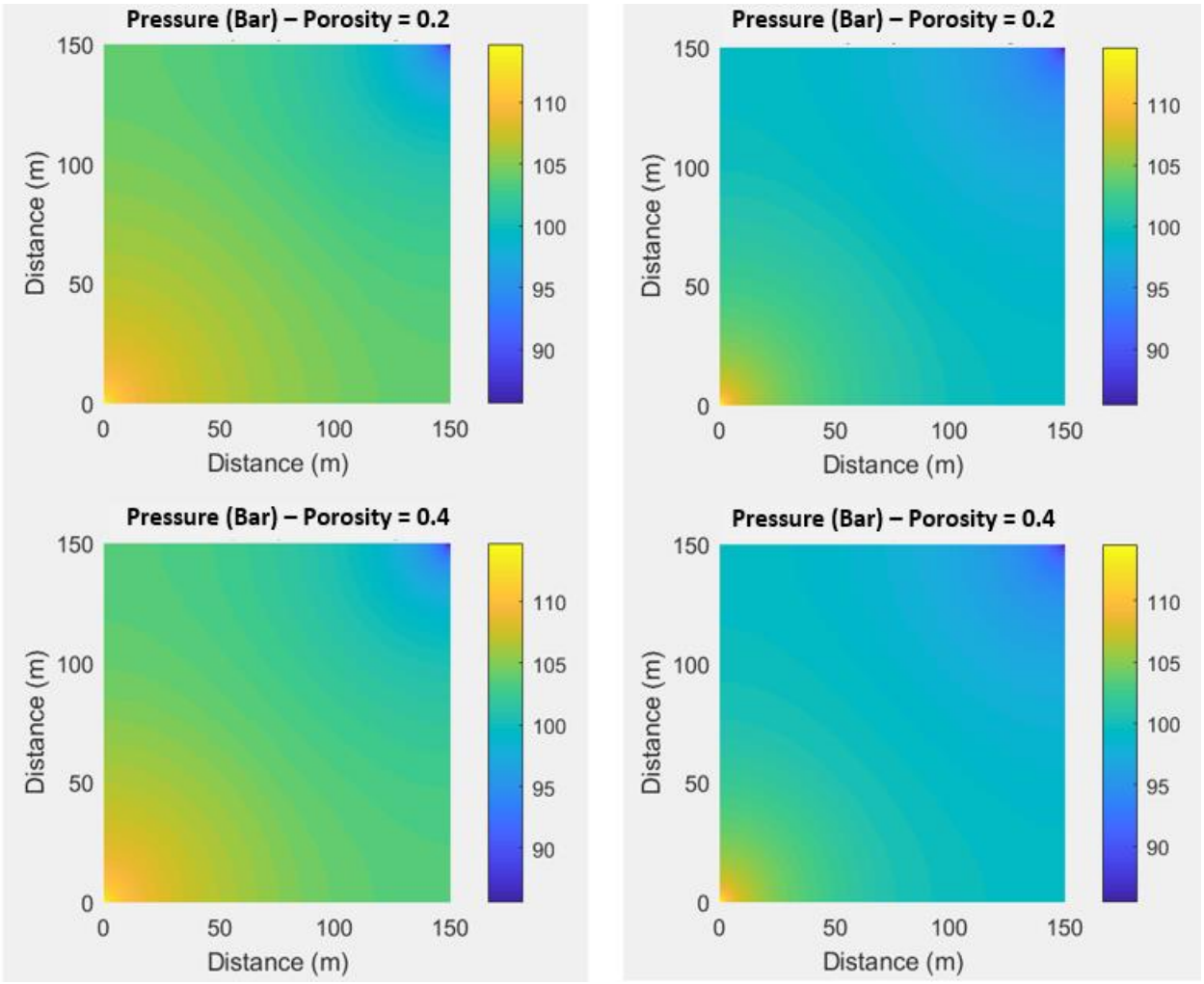

Figure 28: Pressure change results over distance for each porosity for water flood (left) and polymer flood (right)

Pressure change represents oil being displaced. The pressure applied at the injection well was 115 bars with the aim to reach 85 bars when it reaches the production well. Figure 27 shows how for each porosity the pressure at cell [30, 30] was getting affected by the injected pressure to slowly become 115 bars. At cell [30,30] the initial pressure from day 0 represents the pressure of the reservoir before any injection occurs, over the days as water or polymer gets injected with a high pressure, the pressure in cell [30,30] begins to match the pressure of the injected fluid as it

passes that position. It can be seen that the smaller pores has faster pressure change since it is a smaller space and easily gets affected by the passing fluid. For the case of polymer flooding, similar behavior is seen however it changes much slower than the water flooding case and does not change as much in pressure. Figure 28 shows the pressure change over the reservoir starting at 115 at point [0, 0] and slowly spreading into the reservoir. It shows very similar results for all porosities with a vague hint of how the lower porosity pressure is changing faster.

4.5.2 Effect of Reservoir Permeability

A two-dimensional simulation of a sandstone reservoir at 50°C was modelled with 150 m in length, 150 m height and 1 m width. The actual dimension target is 1500m length, 1500m height, and 10m width which was discretized into 150m x150m x1m Cartesian grid cells. As for time, the simulation target run is for 2 years accounting 7 days a week. The rock porosity is 30%. The oil viscosity is 2 cP and its density is 900 kg/m^3. The power used in the Corey correlation of the relative permeability is 2. The pressure at the injecting well is 115 bar and the pressure at the production well is 85 bar. For this simulation, three reservoir permeability values were compared, 0.1 Darcy, 0.3 Darcy and 1 Darcy for both a water flooding case with 1cP viscosity and 1000 kg/m^3 density and a polymer flooding case with 3 cP viscosity that is assumed to behave Newtonian.

4.5.2.1 Reduced Oil Saturation Results

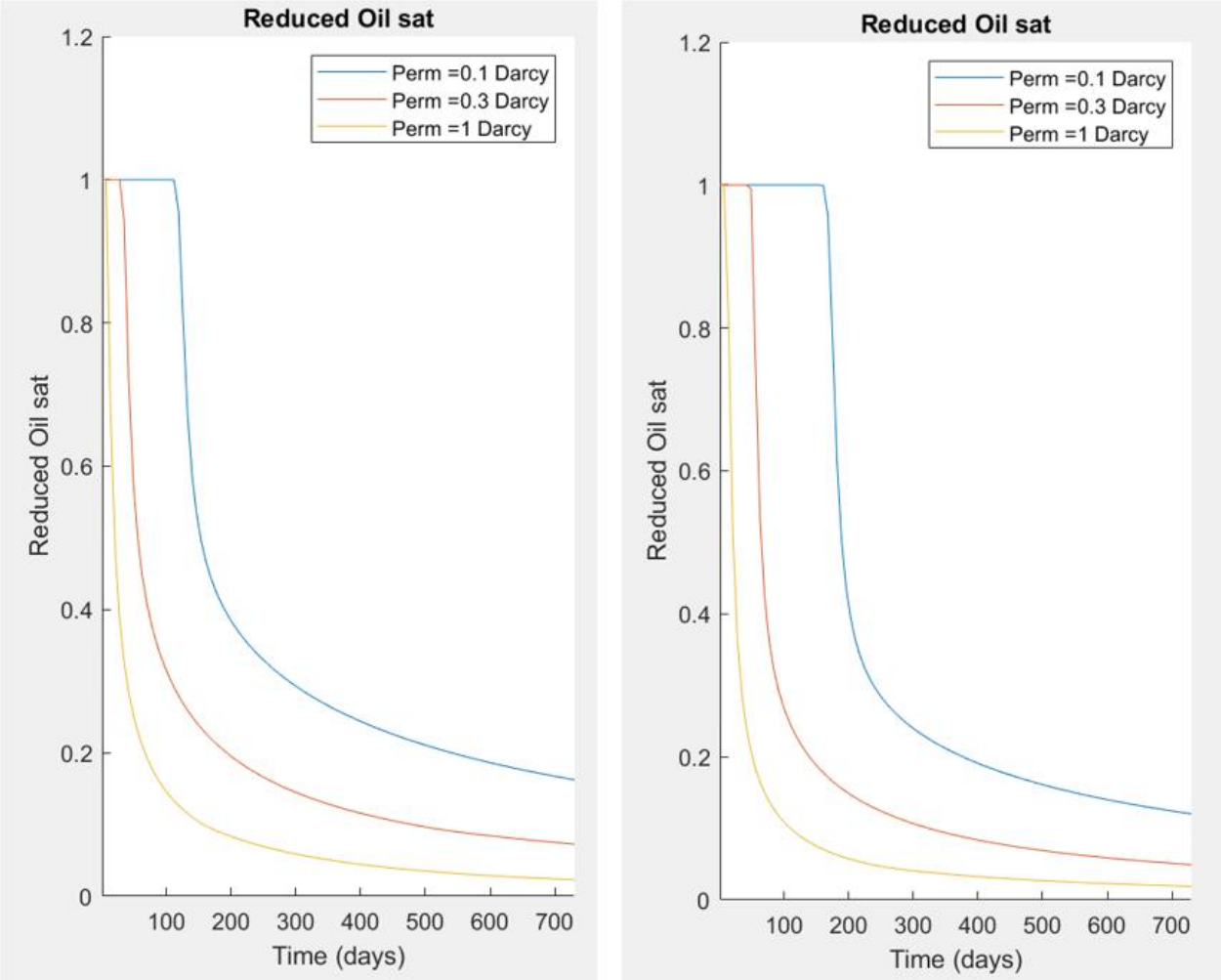

Figure 29: Reduced oil saturation results in cell [30,30] for water flooding (left) and polymer flooding (right) for each permeability

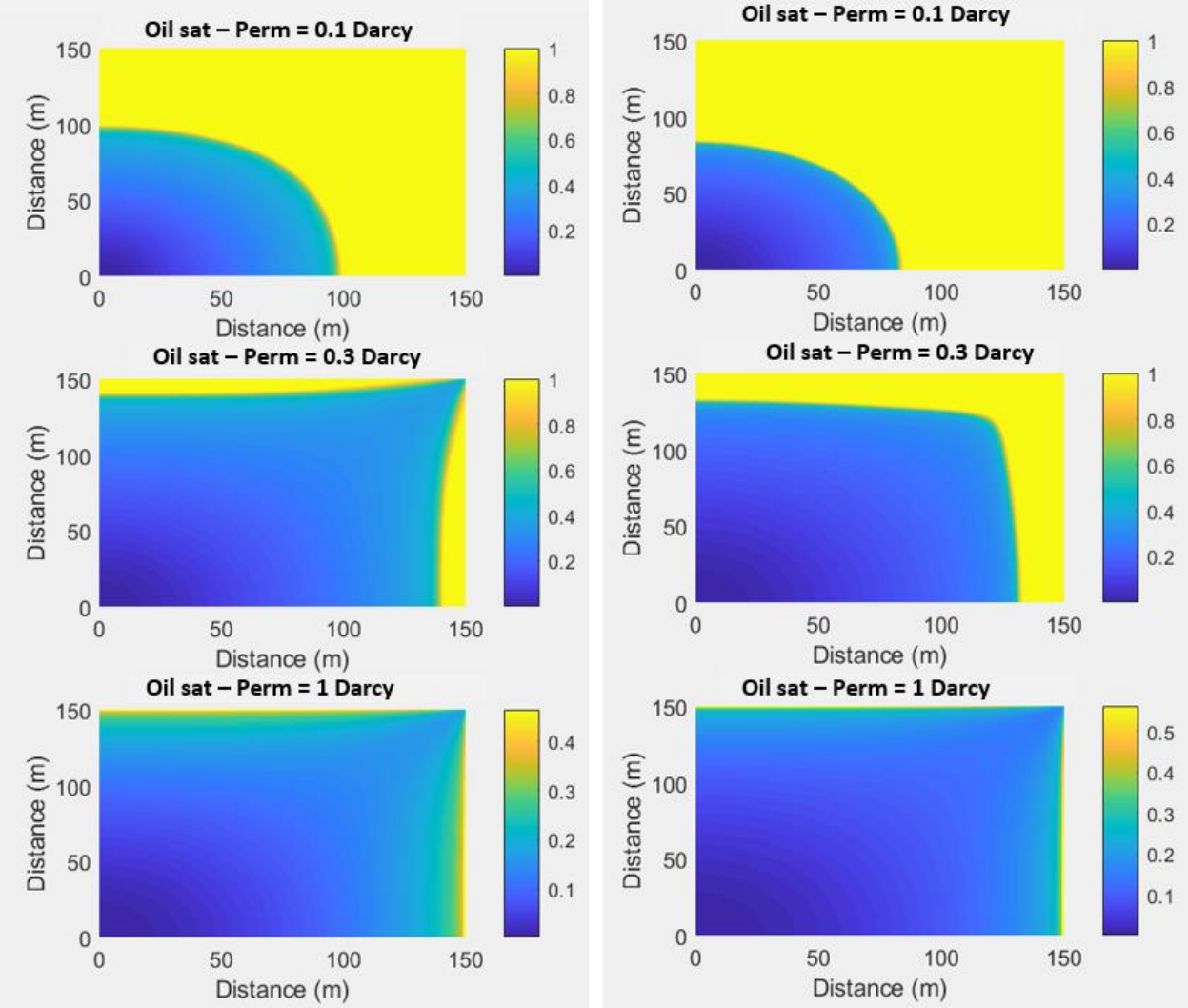

Figure 30: Reduced oil saturation results over distance for each permeability for water flood (left) and polymer flood (right)

Permeability measures the ability of the reservoir to transmit fluids through it. High permeability means the pore spaces are well connected thus the flow of fluids is easier and faster. Figures 29 and 30 demonstrate how with the higher permeability oil saturation decreases faster within the reservoir as its getting displaced. Figure 29 shows how reduced oil saturation is decreased to almost

half its amount around 200 days of operation for the 0.1 Darcy permeability, while the 1 Darcy permeability oil saturation decreased to almost half before even 50 days. Polymer flooding shows the same results but was slower as it takes longer for the viscous polymer solution to displace oil. The overall change in oil saturation over the reservoir for each permeability is clearly shown in Figure 30, the lower the permeability the slower the oil saturation change.

4.5.2.2 Reduced Water Saturation Results

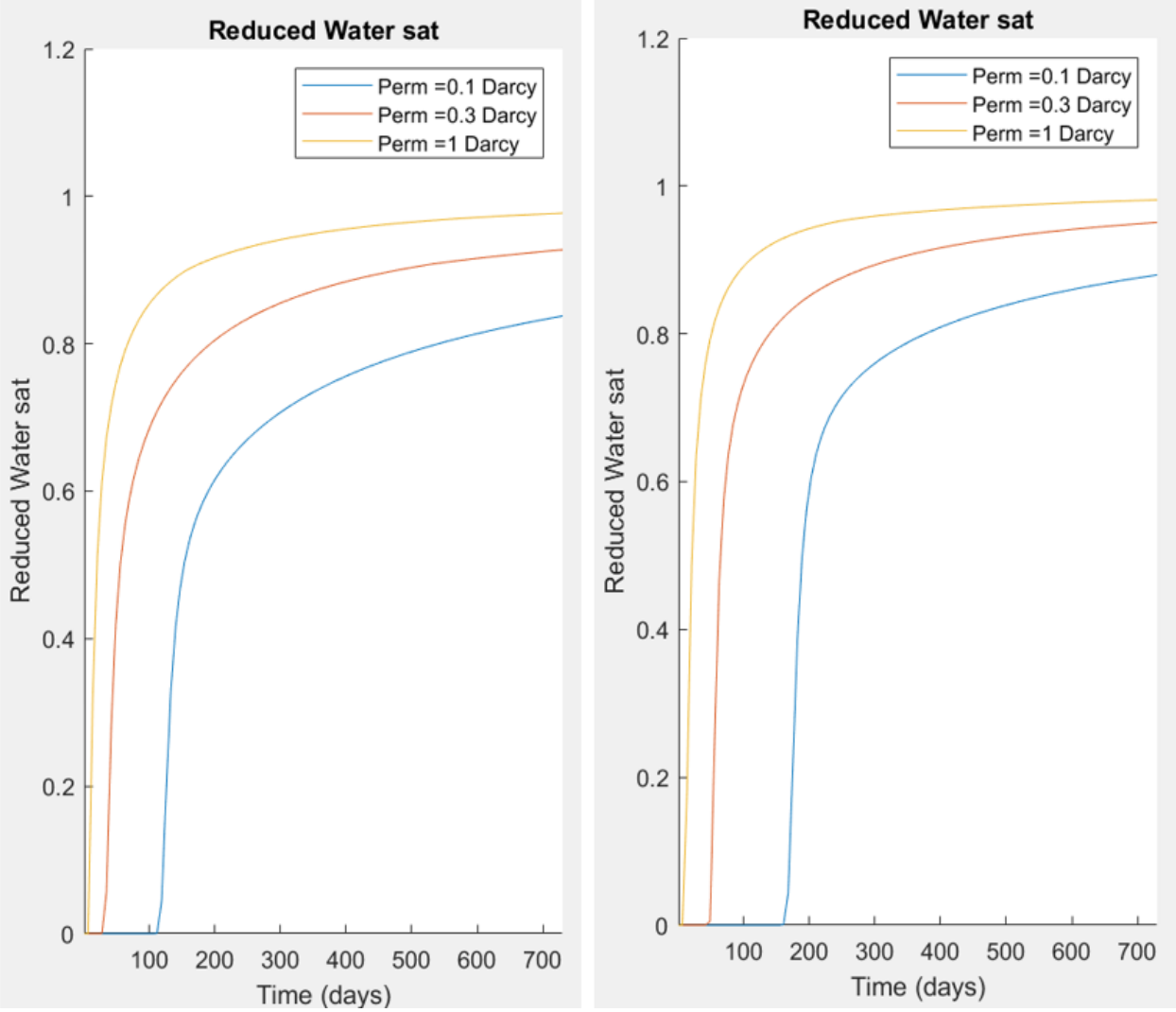

Figure 31: Reduced water saturation results in cell [30, 30] for water flooding (left) and polymer flooding (right) for each permeability

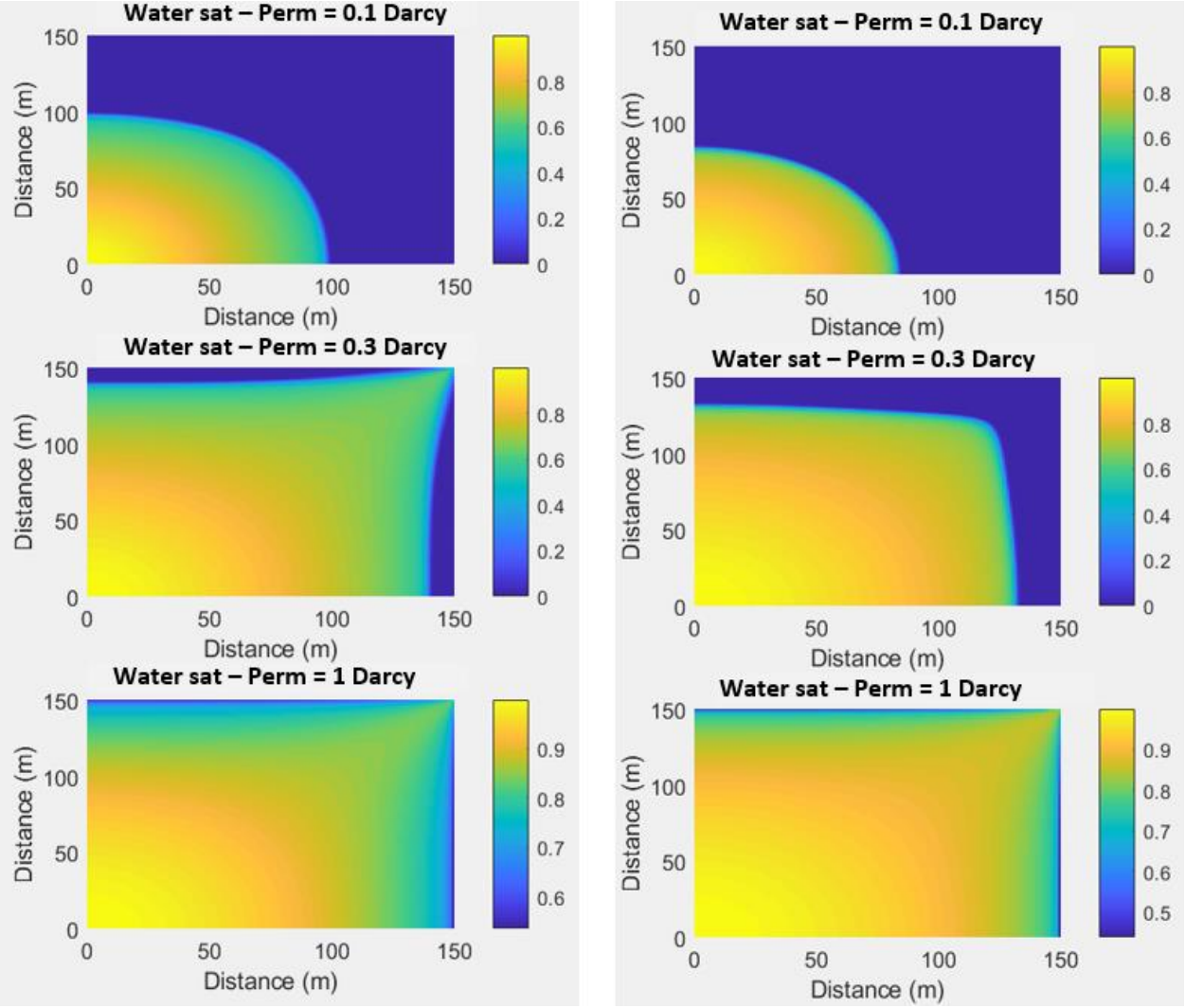

Figure 32: Reduced water saturation results over distance for each permeability for water flood (left) and polymer flood (right)

Figure 31 and 32 illustrate how the reduced water saturation increases faster for a higher permeability value as the flow is easier. As shown in Figure 31, after 200 days, 0.1 Darcy reached a reduced water saturation of 0.6, while 1 Darcy reached a water saturation of 0.9. The viscous polymer solution also increases the water saturation at a highly permeability value.

4.5.2.3 Pressure Change Results

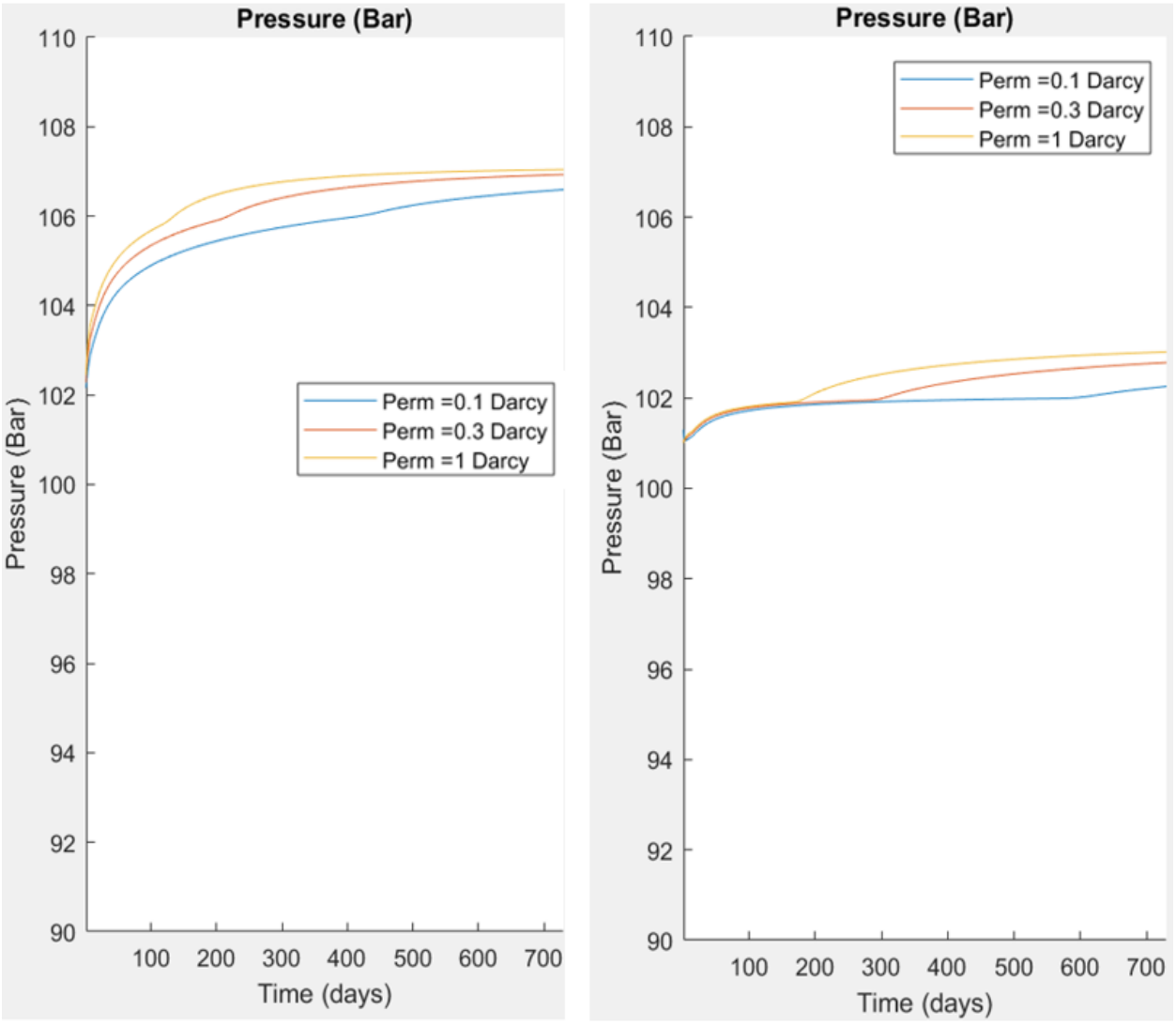

Figure 33: Pressure Change results in cell [30,30] for water flooding (left) and polymer flooding (right) for each permeability

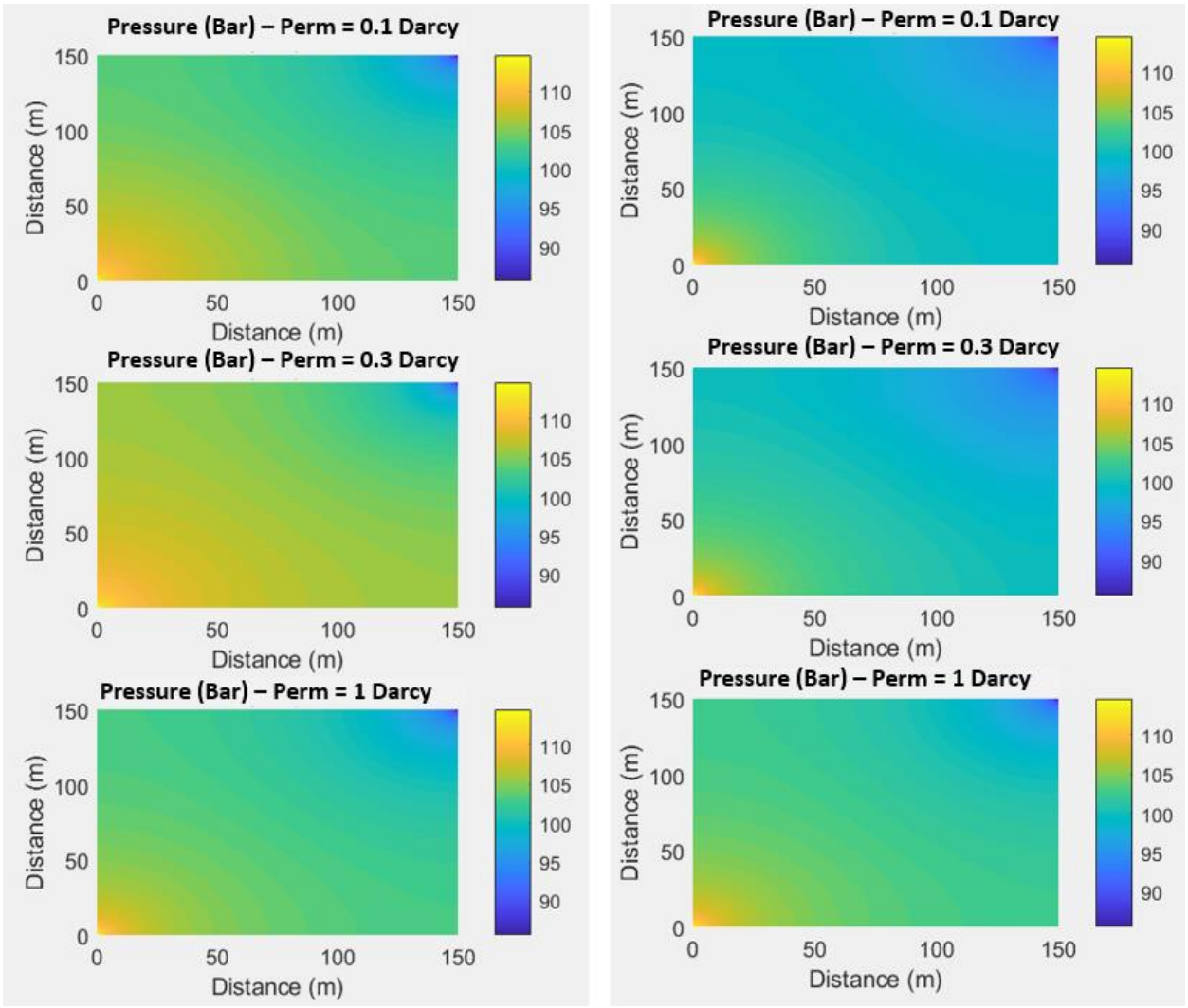

Figure 34: Pressure Change results over distance for each permeability for water flood (left) and polymer flood (right)

As shown in Figures 33 and 34, more pressure change is seen for the more permeable reservoir, indicating more oil displacement is occurring. 1 Darcy reaches around 107 bars, while 0.1 Darcy reaches around 106 bars after 650 days, both starting from 103 bars, hence the highly permeable one had higher pressure change. The polymer flooding case shows a more sluggish representation of the same results with water flooding, however due to its higher viscosity it

takes longer to show any change. The low permeable case requires higher pressure gradient to obtain more energy to produce at the same rate as the high permeable reservoirs.

5. CONCLUSION

The purpose of this thesis was to demonstrate the effectiveness of polymer flooding compared to pure waterflooding by modelling their behavior in the reservoirs simulated. Different cases have been simulated to investigate the results from different perspectives.

The first case was a one-dimensional homogeneous reservoir, where the polymer solution was assumed to be Newtonian fluid and was represented by higher viscosity fluids than water. Results have shown that for the polymer solution, oil saturation increased the fastest at the production well as more oil was being recovered compared to waterflooding. The reduced oil saturation for the polymer flooding reached a total saturation of 1 at 20m into the reservoir, while for the waterflooding the reduced oil saturation reached 0.5 at 40m into the reservoir. For the polymer flooding, the water saturation decreased the fastest at the production well as more water was getting used up to displace the more oil, and pressure decreased the fastest indicating more oil was getting displaced.

The second case was a two-dimensional homogeneous reservoir, where the polymer was still assumed Newtonian. The results from this simulation showed saturation and pressure change at a specific location over the 7 years of operation, as well as their change over the distance within the reservoir. Polymer flooding is more viscous and took longer time than water flooding to get injected and displace oil, however, eventually it achieved the highest saturation and pressure decrease values, indicating more oil was displaced at the end. By the end of the two years operation, the reduced oil saturation in the waterflooding case reached 0.123 and for the polymer flooding, it reached 0.048. This indicates that polymer flooding had more oil displacement.

The third case was a three-dimensional homogeneous reservoir, where a non-Newtonian polymer flooding was compared to pure water flooding. Results have shown that more oil was produced and less water was produced for the polymer flooding, hence oil recovery was enhanced. The black oil case demonstrated how accounting for shear effect can lead to more accurate results for the polymer flooding as shown through the oil and water production plots.

Two reservoir characteristics were investigated to explore their effect on sweep efficiency. Different porosity values were compared (0.2 and 0.4) in a two-dimensional reservoir, for both water flooding and a Newtonian polymer flooding of 3cP viscosity. Results have shown that the higher porosity took longer time to be drained out as the big pores could store more fluid within, thus the reduced oil, water saturation and pressure changes were slow for the higher porosity. Both waterflooding and polymer flooding showed the same behavior, however, for being more viscous the polymer flooding was at a slower pace. The other reservoir characteristic that was investigated in the same two-dimensional reservoir was the reservoir permeability (0.1 Darcy, 0.3 Darcy and 1 Darcy). Results have shown that since the higher permeability means better connectivity between pore spaces, more flow was occurring. Reduced water and oil saturation as well as pressure changes were faster for the higher permeability.

5.1 Recommendations for future work

- Investigate more reservoir characteristics such as temperature or salinity
- Explore the effect of boundary conditions
- Use another software to model polymer flooding vs. water flooding, such as ECLIPSE or CMG STARS
- Examine the effect of reservoir heterogeneity on sweep efficiency

REFERENCES

- Al-Saadi, F.S., Amri, B.A., Nofli, S., Van Wunnik, J., Jaspers, H.F., Harthi, S., Shuaili, K., Cherukupalli, P.K., Chakravarthi, R., 2012. Polymer Flooding in a large field in South Oman – initial results and future plans. SPE 154665 Presented at the SPE EOR Conference at Oil and Gas West Asia Held in Muscat, Oman, April 16–18.
- American Geosciences Institute. (2020). What are the major sources and users of energy in the United States? Retrieved from https://www.americangeosciences.org/tags/2020
- Antoine Thomas (October 19th 2016). Polymer Flooding, Chemical Enhanced Oil Recovery (cEOR) - a Practical Overview, Laura Romero-Zeron, IntechOpen, DOI: 10.5772/64623.
- A.Z. Abidina, , T. Puspasaria , W.A. Nugrohoa. (2012). Polymers for enhanced oil recovery technology.4, 11. doi:10.1016/j.proche.2012.06.002
- Bao, Kai & Lie, Knut-Andreas & MÃ¸yner, Olav & Liu, Ming. (2017). Fully implicit simulation of polymer flooding with MRST. Computational Geosciences. 10.1007/s10596017-9624-
- Buckley. E. S. & Leverett. C. M., Members A.I.M.E, Mechanism of Fluid Displacement in Sands. New York (1941)
- Carpenter, C. (2016, June 1). Polymer Injection in Deepwater Field Offshore Angola. Society of Petroleum Engineers. doi:10.2118/0616-0080-JPT
- Corlay, P., Delamaide, E., (1995). Evaluation and Future of Polymer Injection in the Daqing Field. Institut Français du Pétrole (IFP).
- Corvi P., Heffer K., King P., Tyson S., Verly G., Ehlig-Economides C., Le Nir I., Ronen S., Schultz P., Corbett P., Lewis J., Pickup G., Ringrose P., Guerillot D., Montadert L.,

Ravenne C., Haldorsen H., Hewett T. 1992. Reservoir characterization using expert knowledge, data and statistics. Oilfield Review 4(1):25-31.

- Dake LP. Fundamentals of Reservoir Engineering. The Netherlands, Elsevier Science B.V., 1978
- ENI. SpA (2019). World Oil Review 2019. Volume 1.
- Envirofluid. Oil Recovery Techniques - The need for Enhanced Oil Recovery. (2014).
- Firozjaii, A.M., & Saghafi, H. R. (2019). Review on chemical enhanced oil recovery using polymer flooding: Fundamentals, experimental and numerical simulation. In Petroleum. KeAi Communications Co. https://doi.org/10.1016/j.petlm.2019.09.003
- Guérillot D., Lemouzy P., Galli A., Ravenne Ch. 1990. 3D Fluid Flow Behavior in Heterogeneous Porous Media Characterized by Geostatistical Method, SPE Latin American petroleum engineering conference of the Society of Petroleum Engineers, Rio de Janeiro, Oct. 14-19, Proc., SPE 21081, 8 p.
- Harraz, H.Z., Reservoir heterogeneity | Tanta University (2019).
- IEA. Oil 2020 – Fuel Report Analysis (March 2020).
- IEA. Oil 2018 – Analysis and Forecasts up to 2023 | Fuel Report (March 2018)
- Lie, Knut-Andreas (2019). An Introduction To Reservoir Simulation Using MATLAB/GNU Octave. User Guide for the MATLAB Reservoir Simulation Toolbox (MRST). SINTEF. [Cambridge University Press] DOI:10.1017/9781108591416
- Morel, D. C., Jouenne, S., VERT, M., & Nahas, E. (2008, January 1). Polymer Injection in Deep Offshore Field: The Dalia Angola Case. Society of Petroleum Engineers. doi:10.2118/116672-MS

- Nasr-El-Din, H. A. & and., Taylor, K. C. (1995). Water- soluble hydrophobically associating polymers for improved oil recovery: A literature review. Journal of Petroleum Science and Engineering, 19, 265-280.
- PetroWiki- Capillary Pressure (2016).
- PERM.Inc., TIPM LABORATORY. (2020). Fundamentals of Fluid Flow in Porous Media. Chapter 2. Relative Permeability.
- Preux, C., Malinouskaya, I., Nguyen, Q.-L., & Tabary, R. (2018, June 8). Modeling and Simulating Multi-Polymer Injections. Society of Petroleum Engineers. doi:10.2118/190759-MS
- Schlumberger. (2017). Fundamentals of wettability. Oilfield Review,44
- Schlumberger Oilfield Glossary- The Oilfield Glossary. (2020). Retrieved from https://www.glossary.oilfield.slb.com/
- Seright, R. S. (2016). How much polymer should be injected during a polymer flood? review of previous and Current Practices. 19th European Symposium on Improved Oil Recovery
- Seright, Randall & Campbell, Andrew & Mozley, Peter & Han, Peihui. (2010). Stability of Partially Hydrolyzed Polyacrylamides at Elevated Temperatures in the Absence of Divalent Cations. SPE Journal – SPE J. 15. 341-348. 10.2118/121460-PA
- SINTEF. MRST- Matlab Reservoir Simulation Toolbox. EOR Module (2020).
- SNF Floerger. Enhancing Polymer Flooding Performance – 30 Years of Experience in EOR (September 2012)

- Standnes, D. C. & Skjevrak, I. (2014). Literature review of implemented polymer field projects. Journal of Petroleum Science and Engineering, July 2020. doi:http://dx.doi.org/10.1016/j.petrol.2014.08.24
- Sorbie. K.S. (1991) Polymer-Improved Oil Recovery. Department of Petroleum Engineering. Heriot-Watt University. Springer Science + Business Media, LLC
- Total Foundation. Planète Énergies.The Life Cycle of Oil and Gas Fields (2015); retrieved from https://www.planete-energies.com/en/medias/close/life-cycle-oil-and-gas-fields
- UKOG - Why oil is important.| Energy for Britain (2020); retrieved from https://www.UKOG.com
- Wang, D., Chen, Q., Lu, Z., Feng, Y. et al. (2012). Thermoviscofying polymer used for enhanced oil recovery: Rheological behaviors and core flooding test. DOI: 10.1007/s00289-012-0798-7
- Wang, D., Seright, R.S., Shao, Z. et al. (2008). Key Aspects of Project Design for Polymer Flooding at the Daqing Oil Field. SPEREE 11 (6): 1117-1124. SPE-109682-PA. http://dx.doi.org/10.2118/109682-PA
- Wang, D., Wang, G., and Xia, H. (2011). Large Scale High Visco-Elastic Fluid Flooding in the Field Achieves High Recoveries. Presented at the SPE Enhanced Oil Recovery Conference, Kuala Lumpur, Malaysia, 19-21 July, SPE-144294-MS. http://dx.doi.org/10.2118/144294-MS
- Zendehboudi. S, Bahadori. A (2017) Shale Oil and Gas Handbook. Theories, Technologies, and Challenges. Chapter 8. Pages 285-319. Elsevier. Doi:10.1016/B978-0-12-802100-2.00008-3

- Zerkalov. G., Stanford University. Polymer Flooding for Enhanced Oil Recovery. (2015); retrieved from http://large.stanford.edu/courses/2015/ph240/zerkalov1/